

Observable effects of anisotropic bubble nucleation

Jose J. Blanco-Pillado and Michael P. Salem

*Institute of Cosmology, Department of Physics and Astronomy, Tufts University, Medford,
Massachusetts 02155, USA*

ABSTRACT: Our universe may have formed via bubble nucleation in an eternally-inflating background. Furthermore, the background may have a compact dimension—the modulus of which tunnels out of a metastable minimum during bubble nucleation—which subsequently grows to become one of our three large spatial dimensions. Then the reduced symmetry of the background is equivalent to anisotropic initial conditions in our bubble universe. We compute the inflationary spectrum in such a scenario and, as a first step toward understanding the effects of anisotropy, project it onto spherical harmonics. The resulting spectrum exhibits anomalous multipole correlations, their relative amplitude set by the present curvature parameter, which appear to extend to arbitrarily large multipole moments. This raises the possibility of future detection, if slow-roll inflation does not last too long within our bubble. A full understanding of the observational signal must account for the effects of background anisotropy on photon free streaming, and is left to future work.

Contents

1. Introduction	1
2. Anisotropic bubble nucleation	4
2.1 (2+1+1)-dimensional modulus stabilization	4
2.2 Tunneling instanton and bubble geometry	7
3. Background bubble evolution	9
4. Inflationary perturbations	13
4.1 Power spectrum of a massless scalar	13
4.2 Projection onto spherical harmonics	17
5. Plausibility	23
6. Discussion	25
A. 4d anisotropic tunneling instanton	27
B. Bunch–Davies vacuum	28

1. Introduction

Inflation is generically eternal [1, 2]. That is, for many scalar field potentials the physical volume of inflating spacetime is divergent, with inflation ending only in localized “pockets” within the inflating background. This is the case, for instance, when inflation is driven by the positive vacuum energy of some metastable “parent” vacuum, in which the vacuum phase of our “daughter” universe arises due to tunneling through a potential barrier. The tunneling process is described by an instanton that interpolates between parent and daughter vacua, and appears as bubble nucleation in the inflating spacetime [3, 4]. Indeed this view of cosmology is supported by the present understanding of string theory, which argues for the existence of an enormous landscape of such metastable vacua [5, 6, 7, 8].

In the standard picture, both the parent and daughter vacua have three large (expanding) spatial dimensions. Then the symmetries of the de Sitter parent vacuum suggest the daughter bubble should possess a homogeneous and isotropic geometry—in particular it should possess an $O(3)$ rotational symmetry on any homogeneous foliation [3]. Yet the number of large spatial dimensions may vary from vacuum to vacuum [9, 10, 11, 12], as is expected in string theory.

In particular, one of the large spatial dimensions of the daughter vacuum may be compact in the parent vacuum. The size of this dimension can be characterized by a “volume” modulus that, during bubble nucleation, tunnels out of a metastable minimum, and subsequently grows to very large values. While the resulting bubble is still assumed to reflect the symmetries of the parent vacuum, the presence of the compact dimension breaks $O(3)$ rotational invariance. Indeed, we expect the bubble geometry to be toroidal, with $O(2)$ rotational symmetry in the two large spatial dimensions, uniformly wrapping around the compact space. This would appear as anisotropic initial conditions to an observer in the daughter vacuum.

While the formerly-compact spatial dimension remains globally closed in the daughter bubble, this will not necessarily be evident to a local observer. In order for the daughter vacuum to correspond to our universe, its local evolution should approach an approximately $O(3)$ rotationally-symmetric Friedmann-Robinson-Walker (FRW) cosmology, and the circumference of each large spatial dimension should become and/or remain much larger than the Hubble radius. In fact these conditions are easy to satisfy—the latter is akin to solving the horizon problem of classical big bang cosmology, and is accomplished by a sufficiently long period of slow-roll inflation (after bubble nucleation) along each large spatial dimension [13]. (A period of inflation after bubble nucleation is required even in the standard $O(3)$ -symmetric situation, in order to redshift away the large initial spatial curvature of the bubble.) Meanwhile, it is well known that during such inflation an initially homogeneous but anisotropic universe rapidly approaches local isotropy [14, 15].

Although the initial anisotropy rapidly redshifts away, background anisotropy present at the onset of inflation will generate statistical anisotropy in quantum fluctuations as they expand beyond the Hubble radius, and this in turn can modify the spectrum of primordial density perturbations [16, 17, 18, 19]. During inflation the affected modes are pushed to physical scales far beyond the local horizon; however if the duration of inflation is appropriate they will have re-entered in time to form the largest observable scales in the cosmic microwave background (CMB). Indeed, seemingly anomalous correlations have already been detected among the low-multipole CMB anisotropies [20, 21, 22, 23, 24], which might indicate deviations from statistical isotropy in the inflationary spectrum. (It should be noted that the significance of these “anomalies” is difficult to assess, and their source(s) could be non-cosmological.) In this context a number of models of anisotropy during inflation have been proposed; see e.g. [25, 26, 27, 28, 29, 30, 31, 32, 33]. However unlike other approaches, anisotropic bubble nucleation provides concrete theoretical constraints on the form of initial conditions, and serves as a natural extension of the standard inflationary scenario. Furthermore, it provides an opportunity to confirm aspects of the landscape/multiverse hypothesis.

When the background is homogeneous and isotropic, inflationary perturbations generally decouple into scalar, vector, and tensor modes (for a review of cosmological perturbation theory see e.g. [34]). The same cannot be said for fluctuations about anisotropic backgrounds, which complicates the corresponding analysis. For this reason we assume that metric perturbations are suppressed, until the background geometry of the bubble has become essentially isotropic, after which standard cosmological perturbation theory can be used. As a concrete

model one can imagine the spectrum of isocurvature fluctuations in a sub-dominant scalar field, which are much later converted into adiabatic density perturbations (as in the curvaton mechanism [35]). Note that this simplification comes at little cost: we are interested not in the (model-dependent) amplitude or tilt of the spectrum, but in its statistical anisotropy, and this should not depend strongly on the back-reaction of the scalar on the metric.

Even with this and some other simplifications, the analysis is rather complicated. Although we obtain an analytic expression for the inflationary power spectrum in terms of an appropriate set of anisotropic mode functions, we must resort to numerical evaluation to project this spectrum onto spherical harmonics. Still, we find that certain patterns are evident: whereas the standard (isotropic) picture gives a multipole correlator $C_{\ell\ell'mm'} = \langle \hat{a}_{\ell m} \hat{a}_{\ell' m'}^\dagger \rangle$ that is diagonal in both ℓ and ℓ' and in m and m' , and is independent of m , our scenario introduces off-diagonal components in ℓ and ℓ' (when $\ell - \ell' = \pm 2$), and introduces m -dependence into $C_{\ell\ell'mm'}$ (it is still diagonal in m and m'). (These results are not unlike those of [17], which studied a Bianchi type I anisotropic cosmology.) Our approximations limit us to a region in parameter space where the corrections to $C_{\ell\ell'mm'}$ are suppressed relative to the leading order terms by roughly the present-day curvature parameter Ω_{curv}^0 . While this greatly constrains the size of these effects, they appear to extend to arbitrarily large ℓ , giving hope for statistically significant future detection [36]. Note that because the statistically anisotropic contributions to $C_{\ell\ell'mm'}$ are suppressed by Ω_{curv}^0 .

We have focused on statistical anisotropies in inflationary perturbations, however in this scenario the background spatial curvature of the bubble is itself anisotropic. In particular, the spatial geometry is flat along one direction and open in the two-dimensional planes orthogonal to that direction. While our computation of the inflationary spectrum accounts for this spatial curvature anisotropy, our projection onto spherical harmonics does not. Indeed, anisotropic spatial curvature induces anisotropic expansion, which affects the free streaming of photons and thus deforms the surface of last scattering, along with our perception of angular scales on it [37]. This affects the appearance of the inflationary spectrum, inducing corrections to the observed multipole correlator $C_{\ell\ell'mm'}$. A full understanding of the observable signatures of this model involves combining both of these effects; this is left to future work [38].

The remainder of this paper is organized as follows (an effort has been made to make the major sections self-contained). We study the dynamics of anisotropic bubble nucleation, within the context of a toy model of modulus stabilization, in Section 2. The primary goal of this section is to obtain the instanton boundary conditions that determine the initial conditions for the subsequent bubble evolution. However, because our compactification of one extra dimension with positive vacuum energy is (to our knowledge) novel, we present the model in some detail. In Section 3 we describe the salient features of the post-nucleation, background evolution of the bubble, focusing on the (pre-)inflationary geometry (including obtaining a simple analytic approximation of the metric). In Section 4 we compute the spectrum of inflationary perturbations in a massless scalar field. To better understand the observational signatures of this spectrum, we here also perform a basic analysis of its projection onto spherical harmonics. Some issues pertaining to the plausibility of observing this

scenario are discussed in Section 5. Meanwhile a final summary, including a discussion of various avenues for future work, is provided in Section 6.

Preliminary accounts of this work were presented in [39].

2. Anisotropic bubble nucleation

We study the possibility that our universe formed via bubble nucleation within some parent vacuum in which one of the large spatial dimensions of our vacuum is compact.¹ Although string theory indicates that our vacuum itself has six or seven compact dimensions, for simplicity we consider the associated moduli fields to be non-dynamical spectators in all of the processes of interest here. Thus the parent vacuum is taken to have one compact dimension, the “volume” modulus of which tunnels out of a metastable minimum during bubble nucleation, which subsequently grows to very large size to create our effectively (3+1)-dimensional daughter vacuum. Note that the metastable minimum referred to above must have positive vacuum energy, so the parent vacuum can decay to our positive-vacuum-energy universe.

2.1 (2+1+1)-dimensional modulus stabilization

We first construct an explicit (toy) model of compactification. The model is based on one in [10] (see also references therein). Our purpose is to demonstrate that there are no basic dynamical obstacles to implementing our picture of bubble nucleation, and meanwhile to provide a concrete model for future reference. In order to generate a metastable, positive-vacuum-energy solution for the volume modulus, we use the winding number of a complex scalar field to stabilize the size of the compact dimension. In particular, we consider the (3+1)-dimensional (hereafter denoted 4d) action

$$S = \int \sqrt{-g} d^4x \left[\frac{1}{16\pi G} (R - 2\Lambda) - \frac{1}{2} K(\partial_\mu \varphi^* \partial^\mu \varphi) - \frac{\lambda}{4} (|\varphi|^2 - \eta^2)^2 \right], \quad (2.1)$$

where g is the determinant of the 4d metric $g_{\mu\nu}$, R is the 4d Ricci scalar, Λ is a cosmological constant, and φ is a complex scalar field for which we allow a non-canonical “kinetic” function specified by K . The other terms are constants. Other degrees of freedom, for instance the inflaton and the matter fields of the Standard Model, are assumed to be unimportant during the tunneling process, and are absorbed into Λ (and/or g and R).

The stabilization of the volume modulus of a compact dimension z is most conveniently studied using a metric ansatz with line element

$$ds^2 = e^{-\Psi} \bar{g}_{ab} dx^a dx^b + L^2 e^{\Psi} dz^2, \quad (2.2)$$

¹One might also consider the possibility that two of the large spatial dimensions of our vacuum are compactified in the parent vacuum. In this case the volume modulus couples to the Ricci scalar, but because the (1+1)-dimensional gravity of the non-compact dimensions is conformally invariant, the theory cannot be transformed to the Einstein frame. Although this by itself poses no formal problems to constructing viable models, it does complicate the analysis, and so to retain focus we leave this possibility to future work.

where Ψ represents the modulus field. The effective (2+1)-dimensional (hereafter 3d) metric \bar{g}_{ab} and the modulus Ψ are both taken to be independent of z . Meanwhile, the compact dimension z is defined using periodic boundary conditions, with $0 \leq z \leq 2\pi$, so that it has the topology of a circle with physical circumference $2\pi L e^{\Psi/2}$. Note that we have introduced the following notation. Any quantity defined explicitly within the effective 3d theory (i.e. the theory with the z dimension integrated out), such as the effective 3d metric, is marked with an overline. Whereas Greek indices are understood to run over all dimensions, Latin indices are understood to run over all but the z dimension.

We seek a solution for the scalar field φ that stabilizes the modulus Ψ with respect to small perturbations. The action (2.1) gives the equation of motion

$$\partial_\mu [\sqrt{-g} K' \partial^\mu \varphi] - \sqrt{-g} \lambda \varphi (|\varphi|^2 - \eta^2) = 0, \quad (2.3)$$

where $K' \equiv dK(X)/dX$, with $X = \partial_\mu \varphi^* \partial^\mu \varphi$. Consider for the moment that Ψ is a constant, $\Psi = \Psi_p$. Then the above equation of motion permits the solution

$$\varphi = \left(\eta^2 - \frac{n^2}{\lambda L^2} K' e^{-\Psi_p} \right)^{1/2} e^{inz}, \quad (2.4)$$

where n is an integer, representing the winding number of the phase of φ . Ultimately we are interested in the dynamics of Ψ , in which case Ψ depends on time and (2.4) is no longer an exact solution to the equation of motion. We brush this complication aside by taking

$$\eta^2 \gg \frac{n^2}{\lambda L^2} K' e^{-\Psi}, \quad (2.5)$$

so that to leading order we have $\varphi = \eta e^{inz}$, which in turn gives

$$X \equiv \partial_\mu \varphi^* \partial^\mu \varphi = \frac{n^2 \eta^2}{L^2} e^{-\Psi}. \quad (2.6)$$

Note that we are only interested in dynamics that increase the size of the compact dimension, i.e. dynamics that increase Ψ . Therefore if the above inequality is valid in the parent vacuum, it is valid throughout our analysis (we assume that $K'(X)$ contains no poles in X). The effective 3d action is then obtained by using this solution to integrate the z dimension out of the action. After integrating by parts, this gives

$$S_{3d} = \int \sqrt{-\bar{g}} d^3x \left[\frac{1}{16\pi\bar{G}} \bar{R} - \frac{1}{2} \partial_a \psi \partial^a \psi - \frac{\Lambda}{8\pi\bar{G}} e^{-\alpha\psi} - \frac{1}{2} e^{-\alpha\psi} \bar{K}(X(\psi)) \right], \quad (2.7)$$

where we have defined $\bar{G} \equiv G/(2\pi L)$, $\bar{K} \equiv 2\pi L K$, and $\psi \equiv \Psi/\alpha$, where $\alpha = \sqrt{16\pi\bar{G}}$, with the rescaled modulus ψ being a ‘‘canonical’’ scalar field in the 3d theory.

Recall that our goal is to find a theory/solution in which the modulus ψ is stabilized with positive vacuum energy. The satisfaction of these conditions can be verified by studying the

effective potential of ψ , which corresponds to the last two terms of (2.7). It is sufficient for our purposes to identify a single viable model, so let us propose

$$\overline{K}(X) = 2\pi L (X + \kappa_2 X^2 + \kappa_3 X^3) , \quad (2.8)$$

where κ_2 and κ_3 are constants. Note that it is inappropriate to consider this form of kinetic function as the truncation of a longer series, since we will rely on the various terms being comparable in size. In this sense, (2.8) is ad hoc. The choice $K(X) = 2\beta\sqrt{1+\gamma X} - 2\beta$, with β and γ being constants, may seem more natural, since kinetic terms of this form arise in certain braneworld scenarios. However we have found that this kinetic term does not permit any metastable solutions. Nevertheless, we do not consider this a serious issue. We are here focusing on only one very simple model of compactification, as a representative of the essential dynamics. It seems reasonable to expect that a thorough investigation of, say, the string landscape, would reveal a large number of realistic possibilities.

The 3d effective potential arising due to our choice of $\overline{K}(X)$ is

$$\overline{V}(\psi) = \frac{\Lambda}{8\pi G} e^{-\alpha\psi} + 2\pi L \left(\frac{n^2\eta^2}{2L^2} e^{-2\alpha\psi} + \frac{\kappa_2 n^4\eta^4}{2L^4} e^{-3\alpha\psi} + \frac{\kappa_3 n^6\eta^6}{2L^6} e^{-4\alpha\psi} \right) . \quad (2.9)$$

Let us now explain the choice of \overline{K} leading to the above result. If we had used only the canonical term, $K(X) = X$, then the effective potential would have had no stationary points at finite ψ (recall that we require $\Lambda > 0$). Including the term proportional to κ_2 creates a stationary point for some negative values of κ_2 , but it is always a local maximum. Thus it takes two terms in addition to the canonical one to allow for a local minimum.

The potential $\overline{V}(\psi)$ of (2.9) is displayed in Figure 1 for a particular set of parameter values: $\Lambda/8\pi = 10^{-11}$, $X_0 = n^2\eta^2/L^2 = 10^{-11}$, $\kappa_2 = -X_0^{-1}$, and $\kappa_3 = 0.16X_0^{-2}$ (all quantities are given in units of G). The value of Λ is chosen to roughly correspond to the upper-bound observational limit of the inflationary potential energy in our universe [40], while X_0 is simply chosen to be on the same order as Λ . The other parameters, namely the coefficients that determine κ_2 and κ_3 , were simply guessed by trial and error. Since n , η , and L appear only in the combination $X_0 = n^2\eta^2/L^2$, there is no technical problem with satisfying the inequality (2.5) for any shape of potential $\overline{V}(\psi)$. Also, we have checked that the above values of κ_2 and κ_3 satisfy the ‘‘hyperbolic condition’’ of [41], indicating that the underlying solution for φ is stable to small perturbations.

The effective potential displayed in Figure 1 has a positive vacuum energy local minimum at some value $\psi = \psi_p$. The state with $\psi = \psi_p$ is the parent vacuum, which appears as effectively 3d de Sitter space on scales much larger than $2\pi L e^{\alpha\psi_p/2}$. The daughter vacuum is created when ψ tunnels through the barrier, to some value $\psi = \psi_d$, after which ψ accelerates from rest and rolls down the potential, with $\psi \rightarrow \infty$ as time $x^0 \rightarrow \infty$.

It is important to this work that the daughter vacuum be created via tunneling (Coleman–De Luccia instanton), as opposed to by quantum diffusion over the barrier (Hawking–Moss instanton [42]), because the former gives us a handle on the initial geometry of the daughter

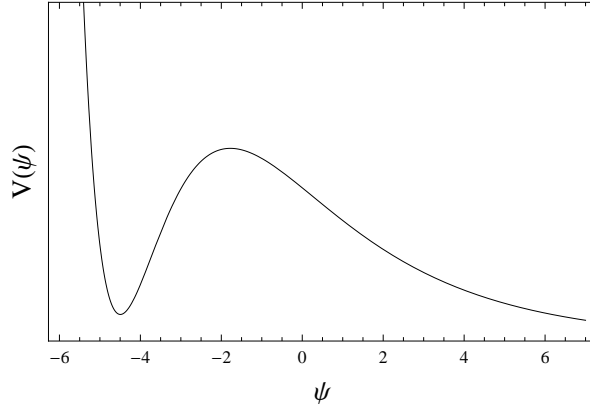


Figure 1: The effective potential of the modulus field ψ ; see text for details.

universe. This translates to the requirement that $|V''| \gtrsim 32\pi G V$ at the peak of the potential barrier. This condition is not hard to satisfy; in particular it is satisfied for the choice of parameters given above. Note that this is not the only channel by which the parent vacuum may decay—in particular it may transition to any vacuum with winding number $n' \neq n$ (see e.g. [10]). Insofar as ψ remains trapped in a local minimum, these transitions are of no interest, as observers like us could never arise in the resulting 3d daughter vacuum. If such a transition eliminates the local minimum or otherwise sets ψ free, then we simply consider it a more sophisticated version of the case we study here.

2.2 Tunneling instanton and bubble geometry

The semi-classical theory of vacuum decay via bubble nucleation is laid out in [3], and we find that we can work in direct analogy to that analysis. The tunneling instanton is found by studying the Euclidean action, and we begin by constructing a metric ansatz that exploits the full symmetry of the parent vacuum. In the 3d effective theory with the compact dimension integrated out, this gives the Euclidean line element

$$ds^2 = d\xi^2 + \rho^2(\xi) [d\chi^2 + \sin^2(\chi) d\phi^2] , \quad (2.10)$$

where ξ is a radial coordinate and χ and ϕ are angular coordinates on a two-sphere of radius $\rho(\xi)$. An effective theory constructed by integrating out a compact dimension is generally valid only on scales much larger than that of the compact dimension. In the present case, however, the tunneling field is also the modulus of the z dimension. If the 4d manifold factorizes as in our ansatz (2.2), then the modulus ψ is independent of z on all scales. Therefore any domain wall of ψ must be independent of z , and there can be no topological structures to support any z dependence of ρ in the tunneling instanton. (These statements hold in particular because the tunneling field is the modulus of the compact dimension; of course such restrictions would not apply to a generic instanton in this background.)

After integrating out the coordinates χ and ϕ (and z), the Euclidean action can be written

$$S_E = 4\pi \int d\xi \left[-\frac{1}{8\pi\bar{G}} (\dot{\rho}^2 + 1) + \rho^2 \left(\frac{1}{2}\dot{\psi}^2 + \bar{V}(\psi) \right) \right], \quad (2.11)$$

where, in the present context, the dot denotes differentiation with respect to ξ . The field equations of the above action can be written

$$\frac{\dot{\rho}^2}{\rho^2} - \frac{1}{\rho^2} = 8\pi\bar{G} \left(\frac{1}{2}\dot{\psi}^2 - \bar{V} \right) \quad (2.12)$$

$$\ddot{\psi} + 2\frac{\dot{\rho}}{\rho}\dot{\psi} = \bar{V}'(\psi), \quad (2.13)$$

where the prime denotes differentiation with respect to ψ . These are the same as the field equations of the standard 4d tunneling instanton, except for some numerical factors [3]. In the present case, the instanton interpolates between a local excitation of the parent vacuum, in which $\psi = \psi_p$, and some point on the opposite side of the potential barrier, at which $\psi = \psi_d$. Inside the daughter vacuum ψ continues to grow, but this evolution is not covered by the tunneling instanton—the geometry of this region is deduced by matching at the instanton boundary, where $\psi = \psi_d$. As a consequence, the circumference of the compact dimension never exceeds $2\pi L e^{\alpha\psi_d}$ in the region covered by the instanton.

It is straightforward to verify the existence of a tunneling instanton by direct numerical integration. The boundary conditions are determined by Taylor expanding $\rho(\xi)$ and $\psi(\xi)$,

$$\rho(\xi) = \xi - \frac{4\pi\bar{G}}{3} \bar{V}(\psi_d) \xi^3 + \dots \quad (2.14)$$

$$\psi(\xi) = \psi_d - \frac{\pi\bar{G}}{3} \psi_d \bar{V}'(\psi_d) \xi^2 + \dots, \quad (2.15)$$

where the coefficients of the expansions are determined using the equations of motion. The value of ψ_d is set by trial and error, so that as ξ approaches some value ξ_{\max} , the instanton smoothly approaches $\psi(\xi) \rightarrow \text{constant}$ (the excited value just prior to tunneling), and likewise $\rho(\xi) \rightarrow \xi_{\max} - \xi$. Of course the details of the instanton depend on the shape of the modulus potential \bar{V} ; to demonstrate the consistency of our model we use the same values of parameters as are used to generate Figure 1. The results of this numerical integration are displayed in Figure 2, and agree with the qualitative description above (note that $\xi = 0$ corresponds to the side of the potential barrier leading into the daughter vacuum). In Appendix A we analyze this tunneling solution from the 4d perspective, substantiating these results.

The instanton displayed in Figure 2 does not appear to be well-described by the so-called thin-wall approximation. Nevertheless, it is not implausible that other modulus potentials exist in which the thin-wall approximation is accurate. In such case the analysis can proceed in exact analogy to that of [3]. Although we do not here propose such a model, we shall assume the tunneling instanton can be well-described by the thin-wall approximation to simplify the computation of inflationary perturbations in Section 4 (Appendix B).

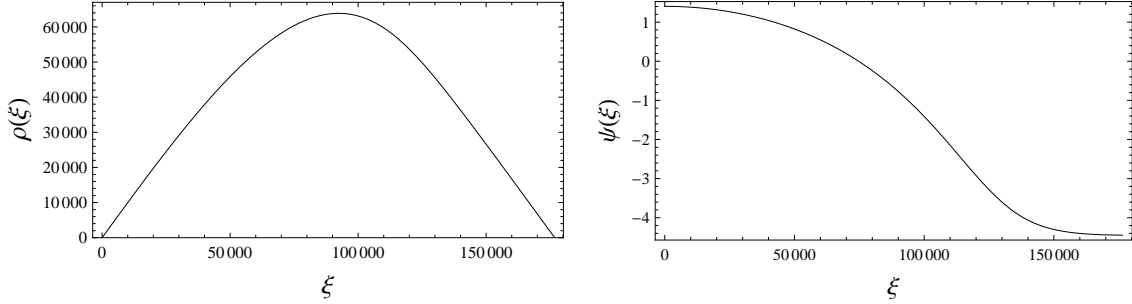


Figure 2: The 3d instanton solution $\rho(\xi)$ (left panel) and $\psi(\xi)$ (right panel), all quantities given in units of G . The large numbers are due to the dynamics being sub-Planckian; see text for details.

Finally, let us note the geometry of the nucleating bubble [3]. In the 3d effective theory, the Lorentzian background geometry is determined by analytic continuation, for instance $\chi \rightarrow i\bar{\chi} + \pi/2$ (and $\xi \rightarrow \bar{\xi}$, $\rho \rightarrow \bar{\rho}$), which generates the line element

$$ds^2 = d\bar{\xi}^2 + \bar{\rho}^2(\bar{\xi}) [-d\bar{\chi}^2 + \cosh^2(\bar{\chi}) d\phi^2] . \quad (2.16)$$

This converts the point $\xi = 0$ into a hypersurface: the future lightcone of the nucleation event (at $\bar{\chi} = 0$). The spacetime can be extended inside this lightcone by analytic continuation, taking $\bar{\chi} \rightarrow \chi - i\pi/2$, $\bar{\xi} \rightarrow i\xi$, and $\bar{\rho} \rightarrow i\rho$. This creates an open FRW bubble interior. After returning the conformal factor $e^{-\Psi} = e^{-\alpha\psi}$ of the original metric ansatz (2.2), and revealing the compact dimension z , the internal bubble geometry has a line element of the form

$$ds^2 = -e^{-\alpha\psi(\xi)} d\xi^2 + e^{-\alpha\psi(\xi)} \rho^2(\xi) [d\chi^2 + \sinh^2(\chi) d\phi^2] + L^2 e^{\alpha\psi(\xi)} dz^2 . \quad (2.17)$$

3. Background bubble evolution

In the previous section we found that bubble nucleation via modulus decay creates an internal bubble geometry corresponding to a (2+1)-dimensional, open FRW manifold crossed with an expanding circle, as given by (2.17). Henceforth we use more traditional geometric variables, with respect to which the line element is written

$$ds^2 = -d\tau^2 + a^2(\tau) [d\chi^2 + \sinh^2(\chi) d\phi^2] + b^2(\tau) dz^2 . \quad (3.1)$$

We now see that the metric is of the Kantowski–Sachs form (case 2 of [43]), a Bianchi type III homogeneous but anisotropic geometry.

To understand the internal dynamics of bubbles like ours, we add to the Lagrangian some matter degrees of freedom. These, we presume, have stress-energy tensor components that are all initially negligible next to those of the inflaton. Furthermore, we presume the inflaton field (initially) reflects the symmetries of the tunneling instanton; in particular we take the inflaton to be static at the instanton boundary and independent of the initially-compact

dimension z . It then suffices to treat the matter as a perfect fluid, with stress-energy tensor $T^\mu_\nu = \text{diag}\{-\rho, p, p, p\}$, where the energy density ρ and pressure density p are (neglecting for the moment quantum fluctuations) functions of time alone. The field equations are then

$$\frac{\dot{a}^2}{a^2} + 2\frac{\dot{a}\dot{b}}{ab} - \frac{1}{a^2} = 8\pi G[V(b) + \rho] \quad (3.2)$$

$$\frac{\ddot{a}}{a} - \frac{\ddot{b}}{b} + \frac{\dot{a}}{a}\left(\frac{\dot{a}}{a} - \frac{\dot{b}}{b}\right) - \frac{1}{a^2} = 8\pi G b V'(b) \quad (3.3)$$

$$\dot{\rho} + \left(2\frac{\dot{a}}{a} + \frac{\dot{b}}{b}\right)(\rho + p) = 0, \quad (3.4)$$

where here and below the prime denotes differentiation with respect to b , the dot differentiation with respect to bubble proper time τ , while the term $V(b)$ is described below. In the second equation, (3.3), we have combined two of the Einstein field equations in order to express a relation that will be useful later.

The anisotropy of the bubble is encoded in the initial conditions for bubble evolution, which are in turn established by the boundary conditions of the tunneling instanton. These set the spatial and time derivatives of all non-metric fields to zero, so at $\tau = 0$ we have

$$\rho = \rho_{\text{inf}}, \quad \dot{\rho} = 0, \quad p = -\rho_{\text{inf}}, \quad \dot{p} = 0, \quad (3.5)$$

where as noted above we assume the initial matter density is dominated by the inflaton. Because the ‘‘volume’’ modulus of the z dimension is the tunneling field, the instanton boundary conditions require that $b(\tau)$ approach a constant as $\tau \rightarrow 0$, i.e.

$$b \rightarrow L e^{\alpha\psi_d/2} \equiv b_d, \quad \dot{b} \rightarrow 0. \quad (3.6)$$

Meanwhile, referring to (2.14) and (2.15) and being careful to track the various variable redefinitions, we find that as $\tau \rightarrow 0$,

$$a \rightarrow 0, \quad \dot{a} \rightarrow 1. \quad (3.7)$$

In Section 2 it was convenient to absorb all of the matter degrees of freedom into the cosmological constant Λ . Moreover, in the 3d effective theory with the z coordinate integrated out, Λ coupled with the modulus ψ in the 3d effective potential $\overline{V}(\psi)$. Now we have returned to the 4d picture, in which Λ is a bare cosmological constant, and have introduced ρ and p to generically characterize the matter content of the universe. Therefore it is convenient to shift the cosmological constant Λ into those quantities. The other ingredients of the (toy) compactification model of Section 2.1 generate a 4d ‘‘potential’’ for b ,

$$V(b) = \frac{1}{2}n^2\eta^2b^{-2} + \frac{\kappa_2}{2}n^4\eta^4b^{-4} + \frac{\kappa_3}{2}n^6\eta^6b^{-6}, \quad (3.8)$$

where we note the change of variable $d\tau = e^{-\alpha\psi/2} dx^0$, which also affects the form of $V(b)$.

For simplicity we treat the inflaton energy density as equivalent to vacuum energy density, $\rho_{\text{inf}} = \text{constant}$. (Thus, according to the above assumptions, ρ_{inf} is almost identical to Λ , the difference being the present dark energy.) It is convenient to also assume the inflaton energy density dominates over the modulus potential, even right after bubble nucleation, i.e. $\rho_{\text{inf}} \gg V(b_d)$. This allows us to obtain the simple analytic solution,

$$a(\tau) = H_{\text{inf}}^{-1} \sinh(H_{\text{inf}} \tau), \quad b(\tau) = b_d \cosh(H_{\text{inf}} \tau), \quad (3.9)$$

where $H_{\text{inf}}^2 \equiv 8\pi G \rho_{\text{inf}}/3$. (Note that the inequality $\rho_{\text{inf}} \gg V(b_d)$ is satisfied by the choice of parameters used to generate Figure 1.) We have chosen the normalization of the scale factor $b(\tau)$ so as to conform to the initial condition given in (3.6).

One might notice that this solution resembles a slicing of 4d de Sitter space. In fact, in the (4+1)-dimensional Minkowski ($ds^2 = -dt^2 + du^2 + dv^2 + dx^2 + dy^2$) embedding:

$$t = H_{\text{inf}}^{-1} \sinh(H_{\text{inf}} \tau) \cosh(\chi) \quad (3.10)$$

$$u = H_{\text{inf}}^{-1} \cosh(H_{\text{inf}} \tau) \cos(b_d H_{\text{inf}} z) \quad (3.11)$$

$$v = H_{\text{inf}}^{-1} \cosh(H_{\text{inf}} \tau) \sin(b_d H_{\text{inf}} z) \quad (3.12)$$

$$x = H_{\text{inf}}^{-1} \sinh(H_{\text{inf}} \tau) \sinh(\chi) \cos(\phi) \quad (3.13)$$

$$y = H_{\text{inf}}^{-1} \sinh(H_{\text{inf}} \tau) \sinh(\chi) \sin(\phi), \quad (3.14)$$

the bubble coordinates $\{\tau, \chi, \phi, z\}$ sit on the hyperboloid $-t^2 + u^2 + v^2 + x^2 + y^2 = H_{\text{inf}}^{-2}$, on which (3.9) gives the scale factors of the induced metric. However this is merely a curiosity; it arises only because we take the limit $\rho_{\text{inf}} \gg V(b_d)$, with $\rho_{\text{inf}} = \text{const}$. Indeed, closer inspection reveals that the Minkowski coordinates u and v are not periodic with the bubble coordinate z (due to the factors of $b_d H_{\text{inf}}$), indicating that the bubble geometry covers only a subset of the hyperboloid, with periodic boundary conditions.²

Note that the bubble geometry features two forms of anisotropy: expansion anisotropy—stemming from the two distinct scale factors a and b —and spatial curvature anisotropy—stemming from the (χ, ϕ) plane being open while the orthogonal z direction is flat. During inflation both forms of anisotropy rapidly redshift away. Although the presence of anisotropy makes choosing the definition of a scalar curvature parameter somewhat ambiguous, we find it convenient to write

$$\Omega_{\text{curv}} \equiv \frac{1}{3a^2 H^2}, \quad (3.16)$$

where $H \equiv \dot{a}/a$ and, following the assumptions above, here and below treat the effect of the modulus potential as negligible next to the above term. Notice that the relationship between

²We can also define the time coordinate $\xi \equiv H_{\text{inf}}^{-1} \sinh(H_{\text{inf}} \tau)$, in which case the line element becomes

$$ds^2 = -(1 + H_{\text{inf}}^2 \xi^2)^{-1} d\xi^2 + \xi^2 [d\chi^2 + \sinh^2(\chi) d\phi^2] + b_d^2 (1 + H_{\text{inf}}^2 \xi^2) dz^2, \quad (3.15)$$

which is also seen as 4d de Sitter space when $b_d^2 = H_{\text{inf}}^{-2}$. Notice that we can now read off the 3d dynamical fields of (2.17): $\rho(\xi) = \xi (1 + H_{\text{inf}}^2 \xi^2)^{1/2}$ and $\psi(\xi) = \alpha^{-1} \ln(1 + H_{\text{inf}}^2 \xi^2)$, with $L = b_d$.

Ω_{curv} and $1/a^2 H^2$ involves a factor of $1/3$ that is not present in the isotropic case. Meanwhile, the expansion anisotropy can be parametrized by

$$h \equiv \frac{\dot{a}}{a} - \frac{\dot{b}}{b}. \quad (3.17)$$

In (3.3) we have combined two of the Einstein field equations so that we can now write

$$\dot{h} + \left(2\frac{\dot{a}}{a} + \frac{\dot{b}}{b}\right)h = \frac{1}{a^2}. \quad (3.18)$$

Thus we see that anisotropic spatial curvature sources anisotropic expansion.

While it would be interesting to understand any observable effects of late-time spatial curvature and expansion anisotropy (some of which have been explored in [44, 45, 46, 47, 37]), for the purpose of this paper we set such questions aside. Indeed, to gain some understanding of the statistical anisotropy of inflationary perturbations in Section 4, we project the spectrum onto a two-sphere “of last-scattering,” treating the background evolution as if the expansion anisotropy h can be ignored. As suggested above and shown in greater detail in [37], this approach is not entirely self-consistent, which is to say the actual surface of last scattering is deformed by the presence of anisotropic expansion h . However the analysis allows us to gain a qualitative understanding of some of the effects of anisotropic bubble nucleation; we leave the more complicated, complete treatment to future work.

For the moment, we simply note two important relationships for later reference. The first is the leading-order comoving distance to the surface of last scattering,

$$\varrho_\star = \int_{\tau_\star}^{\tau_0} \frac{d\tau}{a(\tau)} \simeq \frac{3.5}{a_0 H_0} \simeq 6.1 \sqrt{\Omega_{\text{curv}}^0} \leq 0.50, \quad (3.19)$$

where, to obtain the leading-order expression, we have ignored the effects of spatial curvature and background anisotropy on the evolution of a (we have included the effect of dark energy, modeled as cosmological constant with $\Omega_\Lambda/\Omega_m = 2.85$). Here a subscript “0” designates quantities evaluated at the point of present detection while a subscript “ \star ” designates quantities evaluated at the surface of last scattering, and the last inequality follows from the observational limit $\Omega_{\text{curv}}^0 \leq 6.6 \times 10^{-3}$ (WMAP+BAO+SN with $w = -1$ prior, treating the 95% confidence level as if it were a hard bound) [40]; however it should be emphasized that late-time anisotropic expansion induces a quadrupole in the CMB, itself appearing at order Ω_{curv}^0 , which absent cancellations provides a stronger constraint on Ω_{curv}^0 [37].

The second important relationship comes from realizing that periodicity in one of our large spatial dimensions has not been observed (see e.g. [20]), indicating that the physical circumference of the closed z dimension must be greater than the physical diameter of the surface of last scattering, or

$$2\pi b_\star \geq 2a_\star \int_{\tau_\star}^{\tau_0} \frac{d\tau}{a(\tau)}. \quad (3.20)$$

Ignoring the subleading effect of late-time anisotropic expansion, we see from (3.9) that we can write $b_\star = b_d H_{\text{inf}} a_\star$. Inserting the result of the last paragraph then gives the constraint

$$\Omega_{\text{curv}}^0 \leq 0.27 (b_d H_{\text{inf}})^2. \quad (3.21)$$

Thus, as the quantity $b_d H_{\text{inf}}$ is decreased, the maximum allowed present-day curvature parameter is decreased, along with the size of all related effects. However it should be noted that this result depends crucially on the “redshift factor” $b_d H_{\text{inf}}$ between the two scale factors a and b , which in turn relies on our limit of approximation to obtain the analytic solution (3.7). It is not clear how this constraint is modified outside of the limit $\rho_{\text{inf}} \gg V(b_d)$.

4. Inflationary perturbations

4.1 Power spectrum of a massless scalar

We would like to avoid the formidable task of developing cosmological perturbation theory about the anisotropic background of (3.1). Therefore, we assume that metric perturbations are negligible, until a period when the local background anisotropy is negligible, during which standard cosmological perturbation theory can be used. This could very well be a generic feature of realistic models of inflation, since at least in isotropic models the metric perturbations are suppressed (by the first slow-roll parameter) relative to inflaton fluctuations, until their wavelengths have expanded far beyond the inflationary Hubble radius (see e.g. [48]). However to be concrete and self-consistent we focus on the fluctuations in a subdominant scalar field σ . The fluctuations in σ may be converted into adiabatic density perturbations by a variety of proposed mechanisms; for instance σ could be a curvaton [35]. Because we ignore metric perturbations, we must set aside the interesting question of what modifications to the spectrum of tensor perturbations one might observe in this scenario.

For simplicity we assume that during inflation within the bubble the mass of σ is negligible ($m_\sigma \ll H_{\text{inf}}$), as are the interactions between σ and any other matter fields, so that the only terms involving σ that appear in the Lagrangian are given by

$$S_\sigma = - \int \sqrt{-g} d^4x \frac{1}{2} g^{\mu\nu} \partial_\mu \sigma \partial_\nu \sigma. \quad (4.1)$$

The background metric $g_{\mu\nu}$ is given by (3.1); however we find it convenient here to work in terms of the “conformal” time η_c , where

$$\eta_c \equiv \int \frac{d\tau}{a(\tau)}. \quad (4.2)$$

Note that we use the term “conformal” loosely, as this time parametrization does not make the metric entirely conformally flat. Instead, we have the line element

$$ds^2 = a^2(\eta_c) [-d\eta_c^2 + d\chi^2 + \sinh^2(\chi) d\phi^2] + b^2(\eta_c) dz^2. \quad (4.3)$$

We solve the equation of motion of σ by separation of variables, writing

$$\sigma_{vqrs}(\eta_c, \chi, \phi, z) = \frac{1}{\sqrt{ab}} \Upsilon_{qs}^v(\eta_c) U_{qrs}(\mathbf{x}) = \frac{1}{\sqrt{ab}} \Upsilon_{qs}^v(\eta_c) X_{qr}(\chi) \Phi_r(\phi) Z_s(z), \quad (4.4)$$

where the placement of indices anticipates results below. The factor $(ab)^{-1/2}$ is introduced so that the temporal mode functions Υ_{qs}^v are canonically normalized. The resulting equations for Φ_r and Z_s are very simple:

$$\Phi_r''(\phi) = -r^2 \Phi_r(\phi), \quad Z_s''(z) = -s^2 Z_s(z), \quad (4.5)$$

where here and below we use a prime to denote differentiation with respect to the lone argument of the function that it accents. The factors r^2 and s^2 parametrize the separation of variables. A complete set of orthonormal solutions are

$$\Phi_r(\phi) = \frac{1}{\sqrt{2\pi}} e^{ir\phi}, \quad Z_s(z) = \frac{1}{\sqrt{2\pi}} e^{isz}, \quad (4.6)$$

where the periodic boundary conditions on ϕ and z dictate that r and s must be (positive or negative) integers (recall that we scale the z direction so that it is periodic on $0 \leq z \leq 2\pi$).

Meanwhile, the differential equation for the X_{qr} can be written

$$(1 - c^2) X_{qr}''(c) - 2c X_{qr}'(c) = \left(\frac{1}{4} + q^2 + \frac{r^2}{1 - c^2} \right) X_{qr}(c), \quad (4.7)$$

where the sum $1/4 + q^2$ corresponds to the third separation constant in the above separation of variables. We have defined the variable $c = \cosh(\chi)$ so as to obtain the Legendre equation (as per our convention the primes now denote derivatives with respect to c), the solutions of which are the associated Legendre functions $P_{iq-1/2}^r$ and $Q_{iq-1/2}^r$ [49]. We take interest in the solutions $P_{iq-1/2}^r$, with q real and positive, which are finite and stationary in the limit $c \rightarrow 1$. A convenient normalization is [50]

$$X_{qr}(c) = \frac{\Gamma(\frac{1}{2} + iq - r)}{\Gamma(iq)} P_{iq-1/2}^r(c), \quad (4.8)$$

where Γ denotes the gamma function. The X_{qr} then satisfy the orthonormality condition,

$$\int_1^\infty dc X_{qr}(c) X_{q'r}^*(c) = \delta(q - q'), \quad (4.9)$$

where δ denotes the Dirac delta function. Functions of this sort are studied in [50], and it is straightforward to extend those analyses to the present situation. Using the shorthand $U_{qrs}(\mathbf{x})$ to denote the combined spatial mode functions, one can show that

$$\sum_{r,s} U_{qrs}(\mathbf{x}_1) U_{qrs}^*(\mathbf{x}_2) = \frac{q \tanh(\pi q)}{4\pi^2} \sum_s P_{iq-1/2}(\Xi_{12}) e^{is(z_1 - z_2)}, \quad (4.10)$$

where $\Xi_{12} \equiv \cosh(\chi_1) \cosh(\chi_2) - \sinh(\chi_1) \sinh(\chi_2) \cos(\phi_1 - \phi_2)$. By following the analogous calculation in [50], this ‘‘addition theorem’’ can be used to prove the completeness relation

$$\int_0^\infty dq \sum_{r,s} U_{qrs}(c_1, \phi_1, z_1) U_{qrs}^*(c_2, \phi_2, z_2) = \delta(c_1 - c_2) \delta(\phi_1 - \phi_2) \delta(z_1 - z_2). \quad (4.11)$$

The time evolution of σ is given by the mode functions Υ_{qs}^v , which satisfy

$$\ddot{\Upsilon}_{qs}^v(\eta_c) = - \left(s^2 \frac{a^2}{b^2} + \frac{1}{4} + q^2 - \frac{1}{2} \frac{\ddot{a}}{a} - \frac{1}{2} \frac{\dot{a}\dot{b}}{ab} - \frac{1}{2} \frac{\ddot{b}}{b} + \frac{1}{4} \frac{\dot{a}^2}{a^2} + \frac{1}{4} \frac{\dot{b}^2}{b^2} \right) \Upsilon_{qs}^v(\eta_c). \quad (4.12)$$

To proceed we must specify the (conformal) time dependence of the scale factors a and b . For simplicity we adopt the analytic solution of Section 3, given by (3.9), which treats the inflaton energy density as constant. In terms of this solution, the conformal time is $\eta_c = \ln[\tanh(H_{\text{inf}} \tau/2)]$, which runs from minus infinity to zero as the bubble proper time τ runs from zero to infinity. The two scale factors are then given by

$$a(\eta_c) = -H_{\text{inf}}^{-1} \text{csch}(\eta_c), \quad b(\eta_c) = -b_d \coth(\eta_c). \quad (4.13)$$

Some simplification occurs when we plug this solution into (4.12), and in the end we find

$$\ddot{\Upsilon}_{qs}^v(\eta_c) = - \left[q^2 - 2 \text{csch}^2(\eta_c) + \left(\mu^2 - \frac{1}{4} \right) \text{sech}^2(\eta_c) \right] \Upsilon_{qs}^v(\eta_c), \quad (4.14)$$

where we have defined $\mu \equiv s/b_d H_{\text{inf}}$. The solutions to this equation can be written

$$\begin{aligned} \Upsilon_{qs}^v(\eta_c) &= -2^{-iq} C_1^v \coth(\eta_c) \cosh^{iq}(\eta_c) F \left[-\frac{1}{4} - \frac{iq}{2} - \frac{\mu}{2}, -\frac{1}{4} - \frac{iq}{2} + \frac{\mu}{2}, 1 - iq; \text{sech}^2(\eta_c) \right] \\ &\quad - 2^{iq} C_2^v \coth(\eta_c) \text{sech}^{iq}(\eta_c) F \left[-\frac{1}{4} + \frac{iq}{2} - \frac{\mu}{2}, -\frac{1}{4} + \frac{iq}{2} + \frac{\mu}{2}, 1 + iq; \text{sech}^2(\eta_c) \right] \\ &\equiv C_1^v \mathcal{F}_1(\eta_c) + C_2^v \mathcal{F}_2(\eta_c), \end{aligned} \quad (4.15)$$

where $F \equiv {}_2F_1$ denotes the hypergeometric function [49]. The index v is explained below. We have introduced the shorthand notations \mathcal{F}_1 and \mathcal{F}_2 for later convenience, and have chosen to represent the solutions so that, in the limit $\eta_c \rightarrow -\infty$,

$$\mathcal{F}_1(\eta_c) \rightarrow e^{-iq\eta_c}, \quad \mathcal{F}_2(\eta_c) \rightarrow e^{iq\eta_c}. \quad (4.17)$$

For later reference we also note the asymptotic behavior as $\eta_c \rightarrow 0$,

$$\frac{\mathcal{F}_1(\eta_c)}{\sqrt{a(\eta_c)b(\eta_c)}} \rightarrow \sqrt{\frac{H_{\text{inf}}}{b_d}} \frac{2^{iq} \Gamma(\frac{3}{2}) \Gamma(1 - iq)}{\Gamma(\frac{5}{4} - \frac{iq}{2} + \frac{\mu}{2}) \Gamma(\frac{5}{4} - \frac{iq}{2} - \frac{\mu}{2})} \quad (4.18)$$

$$\frac{\mathcal{F}_2(\eta_c)}{\sqrt{a(\eta_c)b(\eta_c)}} \rightarrow \sqrt{\frac{H_{\text{inf}}}{b_d}} \frac{2^{-iq} \Gamma(\frac{3}{2}) \Gamma(1 + iq)}{\Gamma(\frac{5}{4} + \frac{iq}{2} + \frac{\mu}{2}) \Gamma(\frac{5}{4} + \frac{iq}{2} - \frac{\mu}{2})}. \quad (4.19)$$

The initial conditions for the inflationary perturbations are set by the choice of integration constants C_1^v and C_2^v . Different choices of initial conditions correspond to different choices of the quantum vacuum state [51]—a particularly attractive choice is that of the Bunch–Davies vacuum [52], which maps de Sitter mode functions onto zero-occupation Minkowski wavefunctions in the small-scale limit. Within the context of bubble nucleation in an inflating background, the Bunch–Davies state is determined by tracing the evolution of mode functions back into the parent vacuum and Klein–Gordon normalizing the positive-frequency modes on a Cauchy surface [53, 54, 55]. The analysis is rather tedious, and we relegate it to Appendix B. The results are inserted at an appropriate point below.

Having solved for the mode functions of σ , to obtain the spectrum of inflationary perturbations we promote σ to a quantum operator, $\hat{\sigma}$, and compute the two-point correlation function. The analysis can proceed in exact analogy to the standard formalism (see e.g. [34]). In particular, we can express $\hat{\sigma}$ as a mode expansion of creation and annihilation operators,

$$\hat{\sigma}(\eta_c, \mathbf{x}) = \int dq \sum_{v,r,s} \frac{1}{\sqrt{a(\eta_c)b(\eta_c)}} \left[\Upsilon_{qs}^v(\eta_c) U_{qrs}(\mathbf{x}) \hat{a}_{vqrs} + \Upsilon_{qs}^{v*}(\eta_c) U_{qrs}^*(\mathbf{x}) \hat{a}_{vqrs}^\dagger \right], \quad (4.20)$$

where \hat{a}_{vqrs} and \hat{a}_{vqrs}^\dagger satisfy the appropriate analogues of the standard commutation relations,

$$[\hat{a}_{vqrs}, \hat{a}_{v'q'r's'}^\dagger] = \delta(q - q') \delta_{rr'} \delta_{ss'} \delta_{vv'}, \quad [\hat{a}_{vqrs}, \hat{a}_{v'q'r's'}] = [\hat{a}_{vqrs}^\dagger, \hat{a}_{v'q'r's'}^\dagger] = 0, \quad (4.21)$$

as do the canonical field operator $\sqrt{ab} \hat{\sigma}$ and its conjugate momentum field operator $\hat{\pi}$. The index v is explained in Appendix B; it takes one of two values, which can be denoted \pm . From (4.20) we see that the “Fourier” transform of $\hat{\sigma}(\eta_c, \chi, \phi, z)$ can be written

$$\hat{\sigma}(\eta_c, q, r, s) = \frac{1}{\sqrt{a(\eta_c)b(\eta_c)}} \sum_v \left[\Upsilon_{qs}^v(\eta_c) \hat{a}_{vqrs} - \Upsilon_{(-q)(-s)}^{v*}(\eta_c) \hat{a}_{v(-q)(-r)(-s)}^\dagger \right], \quad (4.22)$$

which gives the equal-time momentum-space two-point correlation function

$$\langle \hat{\sigma}(\eta_c, q, r, s) \hat{\sigma}^\dagger(\eta_c, q', r', s') \rangle = \frac{\sum_v |\Upsilon_{qs}^v(\eta_c)|^2}{a(\eta_c)b(\eta_c)} \delta(q - q') \delta_{rr'} \delta_{ss'}. \quad (4.23)$$

Each “Fourier” mode U_{qrs} associates the set of separation constants $\{q, r, s\}$ with a set of comoving distance scales in the χ, ϕ , and z directions, according to the characteristic scales of variation of $U_{qrs}(\chi, \phi, z)$. After these comoving scales grow larger than the Hubble radius, the mode “amplitude” $\sum_v |\Upsilon_{qs}^v|^2/ab$ rapidly asymptotes to an η_c -independent constant. Because of this, and because all observable scales in our universe first expanded beyond the Hubble radius deep in the inflationary epoch, for practical purposes we can safely evaluate the two-point correlator (4.23) in the limit $\eta_c \rightarrow 0$. This gives the power spectrum

$$\begin{aligned} P_{qs} &\equiv \lim_{\eta_c \rightarrow 0} \frac{1}{a(\eta_c)b(\eta_c)} \sum_v |\Upsilon_{qs}^v(\eta_c)|^2 \\ &= \frac{\pi H_{\text{inf}}}{8 b_d \sinh^2(\pi q)} \left\{ \pi \cosh(\pi q) \left| \Gamma\left(\frac{5}{4} + \frac{iq}{2} + \frac{\mu}{2}\right) \right|^{-2} \left| \Gamma\left(\frac{5}{4} + \frac{iq}{2} - \frac{\mu}{2}\right) \right|^{-2} \right\} \end{aligned} \quad (4.24)$$

$$- \cos(\pi\sqrt{1-\mu^2}) \operatorname{Re} \left[\frac{2^{2iq} \Gamma(\frac{1}{2} - iq - \sqrt{1-\mu^2}) \Gamma(\frac{1}{2} - iq + \sqrt{1-\mu^2})}{\Gamma^2(\frac{5}{4} - \frac{iq}{2} - \frac{\mu}{2}) \Gamma^2(\frac{5}{4} - \frac{iq}{2} + \frac{\mu}{2})} \right] \Bigg\} \quad (4.25)$$

$$\approx \frac{H_{\text{inf}}^2}{2b_d H_{\text{inf}}} (q^2 + \mu^2)^{-3/2}, \quad (4.26)$$

where we have inserted the results from Appendix B. The last relation corresponds to taking the asymptotic limit of large q and μ .³

To begin to understand this result, first note that the separation constant q characterizes comoving radial distance scales in the (χ, ϕ) plane, and thus relates to the standard Cartesian wavenumbers k_x and k_y via $q^2 \sim k_x^2 + k_y^2$ in the flat space (large q) limit. Meanwhile, physical scales in the z direction are redshifted relative to those in the (χ, ϕ) plane due to the dissimilar evolution of the scale factors a and b at early times. The late-time effect is an additional factor of $b(\eta_c)/a(\eta_c)|_{\eta_c \rightarrow 0} = b_d H_{\text{inf}}$ relating physical and comoving distances; therefore we relate the separation constant s to the late-time Cartesian comoving wavenumber k_z via $s \sim b_d H_{\text{inf}} k_z$. Thus the term in parentheses in (4.26) approaches $(k_x^2 + k_y^2 + k_z^2)^{-3/2}$, which gives the standard scale-invariant power spectrum (the factor of $1/b_d H_{\text{inf}}$ will cancel when integrating over wavenumbers to compute observables in the isotropic limit).

Although we have just remarked on the congruence between the asymptotic limit of our result, (4.26), and the result from standard, flat, isotropic inflation, the two inflationary spectra are not the same. The power spectrum (4.26) is expressed in terms of the anisotropic ‘‘Fourier’’ modes $U_{qrs}(\mathbf{x})$, while for instance the isotropic Cartesian Fourier modes are $e^{i\mathbf{k}\cdot\mathbf{y}}$, where $\mathbf{y} = \{y_1, y_2, y_3\}$ are Cartesian coordinates. This difference affects the observed spectrum because the (lack of) correlations implied by the delta functions $\delta(q - q') \delta_{rr'} \delta_{ss'}$ in the two-point correlator (4.23) are different than the (lack of) correlations implied by $\delta^{(3)}(\mathbf{k} - \mathbf{k}')$ in the standard isotropic case.

4.2 Projection onto spherical harmonics

At present the spectrum of primordial density perturbations is most tightly constrained by measurements of fluctuations in the temperature of photons streaming from the surface of last scattering, i.e. CMB fluctuations. It is conventional to use spherical harmonics to cover a two-sphere representing our field of vision (here parametrized by angular coordinates $0 \leq \theta \leq \pi$

³Instead of performing the involved analysis of Appendix B, one might determine the integration constants C_1^v and C_2^v by studying the behavior of Υ_{qs}^v at very early bubble times, $\eta_c \rightarrow -\infty$, and on very small bubble scales, $q \rightarrow \infty$, and equating it with that of a free field in Minkowski space, $\Upsilon_{qs}^v \rightarrow (2q)^{-1/2} e^{-iq\eta_c}$. (Note that the equation specifying Υ_{qs}^v takes the form $\ddot{\Upsilon}_{qs}^v = -q^2 \Upsilon_{qs}^v$ at early conformal times—hence the ‘‘Minkowski’’ wavefunction is independent of s .) This corresponds to choosing the analogue of the so-called ‘‘conformal’’ vacuum, see e.g. [51]. It has the significant drawback of predicting an energy density of fluctuations that diverges as $\eta_c \rightarrow -\infty$, thus converting the mere coordinate singularity at the instanton boundary into a physical singularity. Proceeding nevertheless, in this situation one finds no cause for the index v , and inspecting the asymptotic behavior of \mathcal{F}_1 and \mathcal{F}_2 in (4.17) it is apparent that one would choose $C_1 = (2q)^{-1/2}$ and $C_2 = 0$. The resulting power spectrum is given by the first term of (4.25), but divided by $\coth(\pi q)$. It approaches the same limiting behavior as the Bunch–Davies vacuum, (4.26).

and $0 \leq \phi \leq 2\pi$). The observables are therefore the multipole moments

$$a_{\ell m} = \int d\zeta d\phi Y_{\ell m}^*(\zeta, \phi) \delta_T(\zeta, \phi), \quad (4.27)$$

where δ_T represents the temperature fluctuation and for convenience we have defined $\zeta \equiv \cos(\theta)$. The (orthonormal) spherical harmonics are given by

$$Y_{\ell m}(\zeta, \phi) = \sqrt{\frac{(2\ell + 1)(\ell - m)!}{4\pi(\ell + m)!}} P_{\ell}^m(\zeta) e^{im\phi}. \quad (4.28)$$

The temperature fluctuation δ_T is sourced by density perturbations on the surface of last scattering, but the observed CMB perturbations include secondary effects, which are incurred as photons stream from last scattering to the point of detection. For simplicity we here ignore these effects. In fact, we completely ignore the presence of late-time anisotropic expansion $h \equiv \dot{a}/a - \dot{b}/b$. In this case, null geodesics radiating from the origin of coordinates see a flat metric, equivalent to that of a cylindrical coordinate system. Meanwhile the corresponding flat cylindrical coordinates can be related to flat spherical coordinates, in terms of which the surface of last scattering has fixed radius ϱ_* (again, neglecting h). Thus we obtain

$$\chi_*(\zeta, \phi) = \varrho_* \sqrt{1 - \zeta^2}, \quad \phi_*(\zeta, \phi) = \phi, \quad z_*(\zeta, \phi) = \frac{\varrho_* \zeta}{b_d H_{\text{inf}}}, \quad (4.29)$$

which reflects a particular choice of matching between the cylindrical and the spherical coordinates (recall that $\zeta = \cos(\theta)$). The factor $1/b_d H_{\text{inf}}$ in z comes from the ratio of scale factors a and b when matching onto the isotropic cylindrical coordinates.

We emphasize that while this procedure allows to create a picture of the inflationary spectrum in terms of spherical harmonics, the actual observed spectrum will contain corrections, coming from the anisotropic expansion between the surface of last scattering and the point of present detection. In particular, the presence of anisotropic expansion deforms the surface of last scattering away from the surface defined by (4.29), and perturbs the trajectories of geodesics as they radiate away from the point of observation. Our analysis can be viewed as a first step toward understanding the inflationary spectrum; a more complete analysis of the observational signatures is left to future work.

To be precise, we simply take the temperature fluctuations to be given by

$$\delta_T(\zeta, \phi) \propto \sigma(\eta_c = 0, \mathbf{x}_*(\zeta, \phi)), \quad (4.30)$$

where $\mathbf{x}_* = \{\varrho_*, \zeta, \phi\}$ designates the coordinates of the surface defined by (4.29). Here we have assumed that the isocurvature fluctuations in the light scalar field σ ultimately directly source the adiabatic CMB perturbations, and have ignored a model-dependent proportionality constant. Also, in addition to ignoring the expansion anisotropy h , we have ignored the evolution of primordial perturbations after they enter the Hubble radius.

We are actually interested in the multipole correlation function $C_{\ell\ell'mm'} = \langle \hat{a}_{\ell m} \hat{a}_{\ell'm'}^\dagger \rangle$. Expanding $\sigma(\eta_c = 0, \mathbf{x}_*(\zeta, \phi))$ in terms of mode functions U_{qrs} as in (4.20), we obtain

$$C_{\ell\ell'mm'} = \int d\zeta_1 d\zeta_2 d\phi_1 d\phi_2 dq \sum_{r,s} P_{qs} Y_{\ell m}^*(\zeta_1, \phi_1) Y_{\ell'm'}(\zeta_2, \phi_2) U_{qrs}(\zeta_1, \phi_1) U_{qrs}^*(\zeta_2, \phi_2), \quad (4.31)$$

where P_{qs} is the power spectrum, given by (4.25), and

$$U_{qrs}(\zeta, \phi) = \frac{\Gamma(\frac{1}{2} + iq - r)}{2\pi \Gamma(iq)} P_{iq-1/2}^r \left[\cosh \sqrt{\varrho_\star^2 (1 - \zeta^2)} \right] e^{ir\phi + i\mu \varrho_\star \zeta}, \quad (4.32)$$

where $\mu = s/b_d H_{\text{inf}}$. Plugging the $Y_{\ell m}$ and U_{qrs} into (4.31), we can immediately perform the integrations over ϕ_1 and ϕ_2 . This gives

$$\begin{aligned} C_{\ell\ell'mm'} &= \delta_{mm'} \sqrt{\frac{(2\ell+1)(2\ell'+1)(\ell-m)!(\ell'-m)!}{16\pi^2 (\ell+m)!(\ell'+m)!}} \int d\zeta_1 d\zeta_2 dq \sum_s P_{qs} \\ &\times \left| \frac{\Gamma(\frac{1}{2} + iq - m)}{\Gamma(iq)} \right|^2 P_{iq-1/2}^m \left[\cosh \sqrt{\varrho_\star^2 (1 - \zeta_1^2)} \right] P_{iq-1/2}^{m*} \left[\cosh \sqrt{\varrho_\star^2 (1 - \zeta_2^2)} \right] \\ &\times P_\ell^{m*}(\zeta_1) P_{\ell'}^m(\zeta_2) e^{i\mu \varrho_\star (\zeta_1 - \zeta_2)}. \end{aligned} \quad (4.33)$$

Because of the complexity of this result, we here limit our attention to two basic goals: demonstrating that, as expected, the $C_{\ell\ell'mm'}$ approach the standard, isotropic results in the limit of many e -folds of inflation, and understanding the qualitative features of the low-multipole $C_{\ell\ell'mm'}$ via approximate numerical integrations.

The physical distance to the surface of last scattering is fixed by the late-time big bang expansion history. To model this, we treat the physical distance from the origin to the surface defined by (4.29) as fixed, $a_\star \varrho_\star = \text{constant}$, so that ϱ_\star decreases as the duration of slow-roll inflation increases. Thus, the limit of long-duration inflation corresponds to the limit of very small ϱ_\star . In this limit only modes with large wavenumbers q are relevant to observation, and the normalized Legendre functions approach normalized Bessel functions,

$$\frac{\Gamma(\frac{1}{2} + iq - r)}{\Gamma(iq)} P_{iq-1/2}^r \left[\cosh \sqrt{\varrho_\star^2 (1 - \zeta^2)} \right] \rightarrow \sqrt{q} J_r \left(\varrho_\star q \sqrt{1 - \zeta^2} \right), \quad (4.34)$$

where to be clear J_r is the r th-order Bessel function of the first kind [49], and we ignore the unimportant overall phase. (This result is most easily obtained by taking the appropriate limit of the underlying differential equation.) With this substitution the angular integrations over ζ_1 and ζ_2 can be performed analytically, using a convenient mathematical equality [56]:

$$\int d\zeta e^{i\gamma \cos(\alpha) \zeta} P_\ell^m(\zeta) J_m \left[\gamma \sin(\alpha) \sqrt{1 - \zeta^2} \right] = 2i^{\ell-m} P_\ell^m[\cos(\alpha)] j_\ell(\gamma), \quad (4.35)$$

where j_ℓ denotes the spherical Bessel function of order ℓ [49]. This result holds for positive and negative m , and any $0 \leq \alpha \leq \pi$. Since $P_\ell^{m*} = (-1)^{-m} P_\ell^m$, this equality also holds if we

replace the Legendre polynomial with its complex conjugate on both sides. Note that it is always possible to choose the α and γ of (4.35) so that $\gamma \cos(\alpha) = \pm\mu \varrho_\star$ and $\gamma \sin(\alpha) = q\varrho_\star$, in particular one sets

$$\gamma = \varrho_\star \sqrt{q^2 + \mu^2}, \quad \cos(\alpha) = \frac{\pm\mu}{\sqrt{q^2 + \mu^2}}. \quad (4.36)$$

Putting all of this together, we obtain

$$\begin{aligned} C_{\ell\ell'mm'} &= \delta_{mm'} \sqrt{\frac{(2\ell+1)(2\ell'+1)(\ell-m)!(\ell'-m)!}{\pi^2(\ell+m)!(\ell'+m)!}} i^{\ell-\ell'} \int dq \sum_s q P_{qs} \\ &\times j_\ell\left(\varrho_\star \sqrt{q^2 + \mu^2}\right) j_{\ell'}\left(\varrho_\star \sqrt{q^2 + \mu^2}\right) P_\ell^{m*}\left(\frac{\mu}{\sqrt{q^2 + \mu^2}}\right) P_{\ell'}^m\left(\frac{\mu}{\sqrt{q^2 + \mu^2}}\right). \end{aligned} \quad (4.37)$$

Our next approximation is to replace the sum over integers s with an integral over real $\mu = s/b_d H_{\text{inf}}$. Demonstrating the strict validity of this approximation is tedious; however intuitively we expect it to be accurate at least insofar as $\varrho_\star \ll b_d H_{\text{inf}}$. This is because modes with wavelength $\lambda \sim 1/s$ should not contribute significantly to observables on scales $\varrho \ll \lambda$, and at the same time the discrete spectrum should be well-approximated by a continuum when $s \gg 1$, or $\mu \gg 1/b_d H_{\text{inf}}$. Converting the sum over s into an integral allows us to make use of a convenient variable transformation, defining k and Θ according to

$$q = (k/\varrho_\star) \sin(\Theta), \quad \mu = (k/\varrho_\star) \cos(\Theta), \quad (4.38)$$

where $k \geq 0$ and $0 \leq \Theta \leq \pi$. The Jacobian of the transformation gives $dq d\mu = \varrho_\star^{-2} k dk d\Theta = \varrho_\star^{-2} [k/\sin(\Theta)] dk d\cos(\Theta)$, so that $C_{\ell\ell'mm'}$ can be written

$$\begin{aligned} C_{\ell\ell'mm'} &= \delta_{mm'} \sqrt{\frac{(2\ell+1)(2\ell'+1)(\ell-m)!(\ell'-m)!}{\pi^2(\ell+m)!(\ell'+m)!}} i^{\ell-\ell'} b_d H_{\text{inf}} \int dk d\cos(\Theta) \frac{k^2}{\varrho_\star^3} P_{qs}(k, \Theta) \\ &\times j_\ell(k) j_{\ell'}(k) P_\ell^{m*}[\cos(\Theta)] P_{\ell'}^m[\cos(\Theta)]. \end{aligned} \quad (4.39)$$

After this variable redefinition one can also show that in the limit of small ϱ_\star , the power spectrum approaches $P_{qs}(k, \Theta) \rightarrow (H_{\text{inf}}/2b_d) \varrho_\star^3/k^3$. The integrals over $\cos(\Theta)$ and k can then be performed, giving the standard flat, isotropic result:

$$C_{\ell\ell'mm'}^{(0)} \equiv \lim_{\varrho_\star \rightarrow 0} C_{\ell\ell'mm'} = \frac{H_{\text{inf}}^2}{2\pi \ell(\ell+1)} \delta_{\ell\ell'} \delta_{mm'}. \quad (4.40)$$

Now let us turn to computing some of the low-multipole components of $C_{\ell\ell'mm'}$. The direct numerical estimation of (4.33) converges very slowly, given our limited computational resources. Nevertheless, we can proceed as above, replacing the sum over s with an integral over μ . This by itself does not improve the convergence of the numerical evaluation, however

	$\ell = 2$	$\ell = 3$	$\ell = 4$	$\ell = 5$	$\ell = 6$	$\ell = 7$	$\ell = 8$	$\ell = 9$
$\ell' = \ell$	-1.2	-1.1	-1.0	-1.0	-1.0	-1.0	-1.0	-1.0
$\ell' = \ell \pm 1$	0	0	0	0	0	0	0	0
$\ell' = \ell \pm 2$	0.33	0.35	0.36	0.37	0.38	0.40	0.40	0.40

Table 1: The multipole correlator contrast $\delta C_{\ell\ell'mm'}$ for several values of ℓ and ℓ' , $m = m' = 0$, in units of $\Omega_{\text{curv}}^{(0)}$, using $\varrho_\star = 0.01$ (see the main text for details).

if we now replace the power spectrum P_{qs} of (4.25) with its asymptotic limit (4.26), the integral over μ can be performed analytically,

$$\int_{-\infty}^{\infty} d\mu (q^2 + \mu^2)^{-3/2} e^{i\mu\varrho_\star(\zeta_1 - \zeta_2)} = \frac{2\varrho_\star|\zeta_1 - \zeta_2|}{q} K_1(\varrho_\star q|\zeta_1 - \zeta_2|), \quad (4.41)$$

where K_1 is the (first order) modified Bessel function of the second kind.

As explained above, we expect replacing the sum over s with an integral over μ to be accurate when $\varrho_\star \ll b_d H_{\text{inf}}$. Meanwhile these quantities are observationally constrained by (3.19) and (3.21), which combine to give $\varrho_\star \leq 3.2 b_d H_{\text{inf}}$. Thus there is an interesting region in the parameter space that cannot be probed by this approximation. On the other hand, the asymptotic limit of the power spectrum P_{qs} , (4.26), is approached rapidly as q increases; see Figure 6. We have computed a few elements of $C_{\ell\ell'mm'}$ without this approximation, using $b_d H_{\text{inf}} = 1$ and $\varrho_\star = 0.5$, and the two agree at about the 10% level. Note that, for fixed $b_d H_{\text{inf}}$, the accuracy of these approximations improves as ϱ_\star is decreased.

Putting everything together, our final expression for the $C_{\ell\ell'mm'}$ is

$$\begin{aligned} C_{\ell\ell'mm'} &= \delta_{mm'} \sqrt{\frac{(2\ell+1)(2\ell'+1)(\ell-m)! (\ell'-m)!}{16\pi^2 (\ell+m)! (\ell'+m)!}} \varrho_\star H_{\text{inf}}^2 \int d\zeta_1 d\zeta_2 dq \frac{|\zeta_1 - \zeta_2|}{q} \\ &\times \left| \frac{\Gamma(\frac{1}{2} + iq - m)}{\Gamma(iq)} \right|^2 P_{iq-1/2}^m \left[\cosh \sqrt{\varrho_\star^2 (1 - \zeta_1^2)} \right] P_{iq-1/2}^{m*} \left[\cosh \sqrt{\varrho_\star^2 (1 - \zeta_2^2)} \right] \\ &\times P_\ell^{m*}(\zeta_1) P_\ell^m(\zeta_2) K_1(\varrho_\star q|\zeta_1 - \zeta_2|). \end{aligned} \quad (4.42)$$

To understand the deviations from isotropy, it is convenient to define the quantity

$$\delta C_{\ell\ell'mm'} \equiv \frac{C_{\ell\ell'mm'} - C_{\ell\ell'mm'}^{(0)}}{\max\{C_{\ell\ell'mm'}^{(0)}, C_{\ell'\ell'm'm'}^{(0)}\}}, \quad (4.43)$$

which gives the correction to the ‘‘isotropic background’’ $C_{\ell\ell'mm'}^{(0)}$ of (4.40), in units of a relevant component of $C_{\ell\ell'mm'}^{(0)}$. Note that within the context of the above approximations, the only observable that enters $\delta C_{\ell\ell'mm'}$ is the comoving distance ϱ_\star . Comparing numerical results for several different values of ϱ_\star , we find (roughly) $\delta C_{\ell\ell'mm'} \propto \varrho_\star^2$ when $\varrho_\star \lesssim 1$. Meanwhile (3.19) gives $\varrho_\star^2 \simeq 37\Omega_{\text{curv}}^0$; thus we conclude the non-zero components of $\delta C_{\ell\ell'mm'}$ scale with

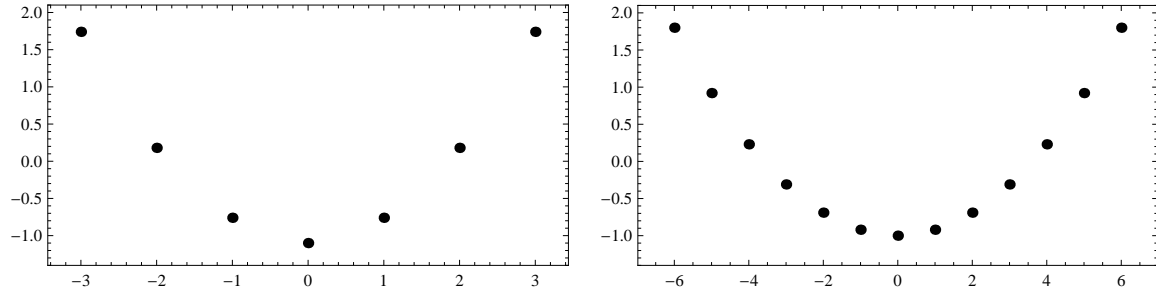


Figure 3: Non-zero values of the the multipole correlator contrast $\delta C_{\ell\ell' mm'}$ for $\ell' = \ell = 3, 6$, in units of $\Omega_{\text{curv}}^{(0)}$, using $\varrho_\star = 0.01$ (see the main text for details).

the present day curvature parameter Ω_{curv}^0 . In Table 1 we display $\delta C_{\ell\ell' mm'}$, in units of $\Omega_{\text{curv}}^{(0)}$, for several values of ℓ and ℓ' , choosing for simplicity $m' = m = 0$, and setting $\varrho_\star = 0.01$.

The most salient feature of Table 1 is the existence of off-diagonal terms with respect to ℓ and ℓ' . This is qualitatively not unlike the results of [17], in which the phenomenology of a Bianchi type I anisotropic universe was studied. As was the case in that scenario, we find that the off-diagonal terms of $C_{\ell\ell' mm'}$ do not fall off very rapidly relative to relevant components of the background $C_{\ell\ell' mm'}^{(0)}$. Indeed, the sequence of $\delta C_{\ell\ell' mm'}$ with $\ell' = \ell \pm 2$ appears to increase with increasing ℓ . Although computing $\delta C_{\ell\ell' mm'}$ at large $\ell' = \ell + 2$ is extremely time consuming, we have explored several values of ℓ' up to $\ell' = 20$ and observed that the sequence asymptotes toward a small constant value, about 0.4 (in units of $\Omega_{\text{curv}}^{(0)}$). We have not displayed components of $\delta C_{\ell\ell' mm'}$ with $\ell' - \ell > 1$ and odd, which we expect, like $\ell' - \ell = 1$, to give precisely zero. The components with $\ell' - \ell > 2$ and even feature very slow numerical convergence, but also appear consistent with zero.

The failure of off-diagonal terms of $\delta C_{\ell\ell' mm'}$ to approach zero in the limit of large ℓ may at first seem to conflict with the usual interpretation that increasing multipole moments ℓ correspond to probing smaller physical scales. To understand this effect, we must recall that we are evaluating the anisotropic modes on a surface that sits at fixed, non-zero ϱ_\star . The asymptotic behavior of (4.34), in which the anisotropic modes converge to isotropic ones, corresponds to the limit $q \rightarrow \infty$, keeping $\varrho_\star q$ constant, which must not be confused with the limit $q \rightarrow \infty$, keeping ϱ_\star constant. In the latter case, there is always a region on the two-sphere (corresponding to large intersection with the open plane) over which there is a discrepancy between the anisotropic and isotropic modes, even in the limit $q \rightarrow \infty$. Since the spherical harmonics receive support over the entire two-sphere (regardless of ℓ), this discrepancy corresponds to statistical anisotropy in the projection onto spherical harmonics. We emphasize that the above comments concern the ratio that appears in $\delta C_{\ell\ell' mm'}$; the observed multipole moments, $C_{\ell\ell' mm'}$, indeed decrease at increasing ℓ and ℓ' .

Table 1 displays results only for when $m' = m = 0$. To illustrate some of the dependence of $\delta C_{\ell\ell' mm'}$ on the indices m and m' , in Figure 3 we plot all of the non-zero entries of $\delta C_{\ell\ell' mm'}$ for $\ell' = \ell = 3$ and $\ell' = \ell = 6$. The qualitative manifestation of statistical anisotropy is evident:

at fixed $\ell' = \ell$, the correction $\delta C_{\ell\ell'mm'}$ increases with increasing magnitude of $m' = m$. The effect is on the same order as the $m' = m = 0$ correction to $\delta C_{\ell\ell'mm'}^{(0)}$. Recall that in standard, isotropic inflation the multipole correlator is independent of m and m' .

Note that because the elements of $\delta C_{\ell\ell'mm'}$ do not fall off very rapidly with increasing ℓ , there is hope to gather sufficient statistics to detect them, despite their being suppressed by roughly the size of the present-day curvature parameter; see e.g. [36]. While we consider it very interesting to explore what are the precise limits placed by cosmic variance on detecting these effects, such an investigation is beyond the scope of the present work.

5. Plausibility

The scenario described in this paper involves the convergence of a number of hypothetical circumstances. Yet many of these ingredients are not crucial to the general idea, which we expect to cover a broad set of models. Furthermore, while the basic framework—bubble nucleation via modulus destabilization followed by not much more inflation than is necessary to flatten our Hubble volume—is certainly speculative, we do not consider it extremely implausible. We here take a moment to justify these attitudes.

An essential ingredient of our model is that the vacuum in which our bubble nucleates has one fewer large spatial dimensions than that of our universe. A toy model to implement this is described in Section 2.1; however we consider this model only as a simple illustration of the concept. If we accept ten- or eleven-dimensional string theory as a fundamental description of nature, then the existence of our (3+1)-dimensional pocket is proof of the compactification principle, and it seems reasonable to presume that other compactifications are possible and that quantum transitions among them occur during eternal inflation.

The mere occurrence of such transitions does not imply that one is likely to be the progenitor of our universe. One might argue that, all else being equal, the nucleation of our bubble in a vacuum with a greater number of large (expanding) spatial dimensions is more likely, because of the greater physical volume available to nucleate a bubble. However, this statement involves an assumption about the spacetime measure on the multiverse, raising an unresolved issue in the understanding of eternal inflation. We now briefly explain.

One consequence of eternal inflation is that the number of bubble nucleations (or of any type of event) diverges with time. Indeed, the physical three-volume on an FRW foliation within a given bubble diverges as well. Attempts to regulate these divergences have revealed that cosmological predictions tend to depend on the choice of regulator—this is known as the measure problem (for some reviews see e.g. [57, 58]). While it is unclear what is the correct measure on the multiverse, certain measures can be ruled out for making predictions in wild disagreement with our observations. In particular, measures that grant greater weight according to larger inflationary expansion factors suffer from the “ Q -catastrophe” (and “ G -catastrophe”) [59, 60, 61], predicting the amplitude of primordial density perturbations and the gravitational constant to be in stark conflict with what is observed. Thus, one should be

skeptical of arguments about the frequency of events in the multiverse based only on naive comparisons of inflationary expansion factors.

In fact, the question of how the spacetime measure should address transdimensional tunneling in the multiverse has not yet been addressed in the literature. To support the attitude expressed above, we here briefly speculate about three of the leading measure proposals. One of these is the comoving probability measure [62, 63], which can be seen as weighting events according to the frequency at which they are encountered by the future histories of a given worldline. A simple generalization is to specify the worldline including its position in any initial compact dimensions, in which case this measure would not grant any additional weight to parent vacua simply because they have a greater number of expanding dimensions. The generalization of the causal patch measure [64] is less clear, but since it also counts events according to their proximity to the future histories of a given worldline (specifically, whether or not they reside in the surrounding causal patch), one might guess that it would not give a very different result. The scale-factor cutoff measure [63, 65] counts events only if they reside in the finite volume between an initial spacelike hypersurface and a later hypersurface determined by a fixed amount of expansion. One way to extend this measure to the case of transdimensional tunneling is to track the density of a fiducial “dust” of test particles scattered over the initial hypersurface, including over any compact dimensions, defining the later hypersurface according to when the density drops below a pre-specified value. In this case, the extra volume due to an additional expanding dimension would be canceled by the extra dilution of the dust due to that expansion, and again parent vacua receive no additional weight simply due to having a greater number of expanding spatial dimensions.

It is not enough to have an effectively (2+1)-dimensional parent vacuum nucleate a bubble of our vacuum phase—we also require an appropriate period of slow-roll inflation subsequent to bubble nucleation. The analysis of this paper introduces a number of assumptions about this period of inflation, but we consider all but one to be simple matters of convenience. For example, we assumed that the inflaton energy density is precisely constant during inflation, and that density perturbations are sourced by fluctuations in a second, subdominant field. Yet we expect these choices to affect only the amplitude and tilt of the resulting spectrum of perturbations, both of which are model-dependent parameters that can presumably be tuned to match observation by simply picking an appropriate implementation of inflation.

We also assumed that the inflaton energy density dominates over the modulus effective potential immediately after bubble nucleation. This was essential to obtaining a simple analytic solution for the background metric during inflation, but with hindsight we can see this too is not an important assumption. The balance of contributions to the energy density in the bubble affects only the time dependence of the scale factors a and b , which in turn affects only the power spectrum P_{qs} (not the anisotropic “Fourier” mode functions U_{qrs}). The effect of anisotropy in the power spectrum was found to be subdominant to that coming from the mode functions; indeed the anisotropy of the power spectrum is ignored in the results of Section 4.2, since this allowed us to introduce an additional approximation to speed the numerical integration given our limited computational resources.

The crucial assumption is that slow-roll inflation lasts long enough to conform to present observation, but not so long as to push all of the effects of initial anisotropy outside of our present horizon. This requires a sort of “fine-tuning” between the inflaton potential and the present age of the universe, which, at first glance, seems to involve an unusual coincidence. However, such a “coincidence” may find an explanation in landscape cosmology.

If indeed our pocket is one among a diverging set in an eternally expanding multiverse, then we must be careful to account for all of the selection effects that modulate the likelihood for us to make a given observation. These selection effects are ultimately encapsulated in the choice of spacetime measure; however in the present case it turns out that all three measures mentioned above give similar predictions [66, 67, 68, 69]. Roughly speaking, there is a factor—called the “prior”—which gives the relative probability that a random spacetime point resides in a bubble that undergoes N e -folds of slow-roll inflation. This is convoluted with a second factor—called the “anthropic factor”—which is proportional to the density of (appropriately defined) observers in bubbles characterized by N e -folds of inflation.

The prior distribution is addressed in [66], where an (admittedly crude) argument is given to suggest that the landscape might strongly prefer fewer e -folds of slow-roll inflation, with the distribution $dP(N) \propto N^{-4} dN$. The effect of anthropic selection is most carefully computed in [69], where it is found that the mass function of Milky-Way mass galaxies is approximately independent of Ω_{curv} for $\Omega_{\text{curv}} \ll \mathcal{O}(0.1)$, and falls off exponentially for roughly $\Omega_{\text{curv}} > 0.7$ (note that $\Omega_{\text{curv}} \propto e^{-2N}$ with a proportionality constant that depends on the scale of inflation and some details of reheating and the subsequent big bang evolution). The combination of these effects places most observers in spacetime regions in which Ω_{curv}^0 is unobservably small (i.e. below cosmic variance), but at the same time gives a reasonable probability, roughly of order ten percent chance, to observe $\Omega_{\text{curv}}^0 \gtrsim 10^{-5}$ [68, 69].

6. Discussion

The present understanding of string theory and inflationary cosmology points to a picture of spacetime containing countless bubbles endlessly nucleating within an eternally-inflating background. In the context of the string landscape, the complete set of bubbles contains a wide range of low-energy physics, including different numbers of compact dimensions (in fact it is the enormous variety of compactifications that inspires the diversity of the landscape in the first place). It is therefore a priori possible that our bubble, containing three large (expanding) spatial dimensions, nucleated within a vacuum containing only two such dimensions.

For instance, the eternally-inflating vacuum in which our bubble nucleates could contain a compact dimension, the size of which is governed by a metastable modulus that tunnels through a potential barrier upon bubble nucleation. The tunneling instanton and initial bubble geometry then respect reduced symmetry from the (3+1)-dimensional perspective, due to the presence of the additional compact dimension. Yet, as expected, a round of slow-roll inflation within the bubble is sufficient to redshift away the initial anisotropy and curvature, creating an $O(3)$ -symmetric FRW cosmology consistent with the observed universe.

Nevertheless, if inflation within the bubble does not last too long, effects of the initial anisotropy may be observable. We here focus on one such effect: the generation of statistical anisotropy among large-scale inflationary perturbations. We find that, when projected onto a two-sphere approximating the surface of last scattering, the inflationary spectrum generates a multipole correlator $C_{\ell\ell'mm'}$ that features (in an appropriate coordinate system) off-diagonal elements in ℓ and ℓ' (when $\ell - \ell' = \pm 2$), as well as dependence on the multipole moment m (it is still diagonal in m and m'). These effects are suppressed relative to the statistically-isotropic components of $C_{\ell\ell'mm'}$ by the present-day curvature parameter Ω_{curv}^0 , but appear to extend to arbitrarily large ℓ .

There are a number of remaining issues to be explored. Most importantly, as a first approach to the problem we have ignored the effects of spatial curvature and expansion anisotropy on the free streaming of photons from the surface of last scattering to the point of present detection. In fact, anisotropic spatial curvature sources anisotropic expansion, which in turn deforms the surface of last scattering away from the surface on which we project the inflationary spectrum, in addition to perturbing the trajectories of geodesics as they radiate away from the point of observation. A full understanding of the observable signatures of anisotropic bubble nucleation requires combining both of these effects.

Also, we have ignored metric perturbations, focusing on the spectrum of a subdominant scalar field and assuming its isocurvature perturbations translate directly into adiabatic density perturbations. While we do not expect this to have a large effect on the spectrum of statistical anisotropies (compared to for instance the standard scenario where the primordial perturbations are sourced by the inflaton itself), it does not allow us to study the tensor perturbations generated during inflation. Because scalar and tensor metric perturbations in general do not decouple in an anisotropic background, there are possibly interesting correlations between these signals. Ignoring metric perturbations also hides any interesting effects that might come from fluctuations in the bubble wall itself.

It would also be interesting to explore the nature and degree of non-Gaussianity implied by the existence of statistical anisotropy among inflationary perturbations.

Finally, another potential signature of multiverse cosmology is observable bubble collisions, see e.g. [71, 72, 73, 74, 75]. It would be interesting to understand whether the reduced symmetry at early times of anisotropic bubble nucleation affects the spectrum of bubble collisions on typical observer's sky, or if there is any special signature of collisions with bubbles containing a reduced number of large spatial dimensions [76].

Acknowledgments

The authors thank Belen Barreiro, Raphael Bousso, Frederik Denef, Ben Freivogel, Jaume Garriga, Lam Hui, Matthew Johnson, Matthew Kleban, Ken Olum, Leonard Susskind, Vitaly Vanchurin, and Alexander Vilenkin for helpful discussions. JJB-P and MPS are supported by the U.S. National Science Foundation, under grants 06533561 and 0855447, respectively.

Note added: We very recently became aware of interesting work by another group, which computes the effect of late-time spatial curvature and expansion anisotropy on photon free-streaming from the surface of last scattering [77].

A. 4d anisotropic tunneling instanton

We here verify the description of the tunneling instanton in the 3d effective theory of Section 2.2, by solving for the corresponding solution in the full, anisotropic 4d geometry. Our starting point is the 4d action, (2.1). The 4d line element of the parent vacuum can be written

$$ds^2 = d\sigma^2 + a^2(\sigma)[-dt^2 + \cosh^2(t) d\phi^2] + b^2(\sigma) dz^2, \quad (\text{A.1})$$

and as before we study the approximate complex-scalar-field solution $\varphi = \eta e^{inz}$. Taking account of the energy momentum tensor of this model,

$$T_{\mu\nu} = K' \partial_\mu \varphi^* \partial_\nu \varphi + g_{\mu\nu} \left(-\frac{1}{2} K(X) - \frac{\lambda}{4} (|\varphi|^2 - \eta^2)^2 - \frac{\Lambda}{8\pi G} \right), \quad (\text{A.2})$$

where $X \equiv \partial_\mu \varphi^* \partial^\mu \varphi = n^2 \eta^2 b^{-2}$ and $K' \equiv dK/dX$, we obtain the equations of motion,

$$\frac{\dot{a}^2}{a^2} + 2 \frac{\dot{a}\dot{b}}{ab} - \frac{1}{a^2} = -8\pi G \left(\frac{n^2 \eta^2}{2b^2} + \frac{\kappa_2 n^4 \eta^4}{2b^4} + \frac{\kappa_3 n^6 \eta^6}{2b^6} \right) - \Lambda \quad (\text{A.3})$$

$$2 \frac{\ddot{a}}{a} + \frac{\dot{a}^2}{a^2} - \frac{1}{a^2} = 8\pi G \left(\frac{n^2 \eta^2}{2b^2} + \frac{3\kappa_2 n^4 \eta^4}{2b^4} + \frac{5\kappa_3 n^6 \eta^6}{2b^6} \right) - \Lambda. \quad (\text{A.4})$$

Above we have used $K(X) = X + \kappa_2 X^2 + \kappa_3 X^3$ as in the main text. These equations of motion permit a solution of the form

$$a(\sigma) = H_p^{-1} \sin(H_p \sigma), \quad b(\sigma) = b_p, \quad (\text{A.5})$$

with H_p and b_p being constants, provided that we impose the condition,

$$\frac{\Lambda}{8\pi G} + \frac{n^2 \eta^2}{b^2} + \frac{3\kappa_2 n^4 \eta^4}{2b^4} + \frac{4\kappa_3 n^6 \eta^6}{2b^6} = 0, \quad (\text{A.6})$$

the solution of which is b_d . The constant H_p is then given by

$$H_p^2 = 8\pi G \left(\frac{n^2 \eta^2}{2b_d^2} + \frac{\kappa_2 n^4 \eta^4}{2b_d^4} + \frac{\kappa_3 n^6 \eta^6}{2b_d^6} \right) + \Lambda. \quad (\text{A.7})$$

In the language of the 3d effective theory, this condition can be written $\bar{V}' = 0$; therefore we have identified the compactification solution but from the vantage of the full 4d theory. As expected, inserting this solution into (A.1) gives the line element of (2+1)-dimensional de Sitter space crossed with a fixed-circumference circle.

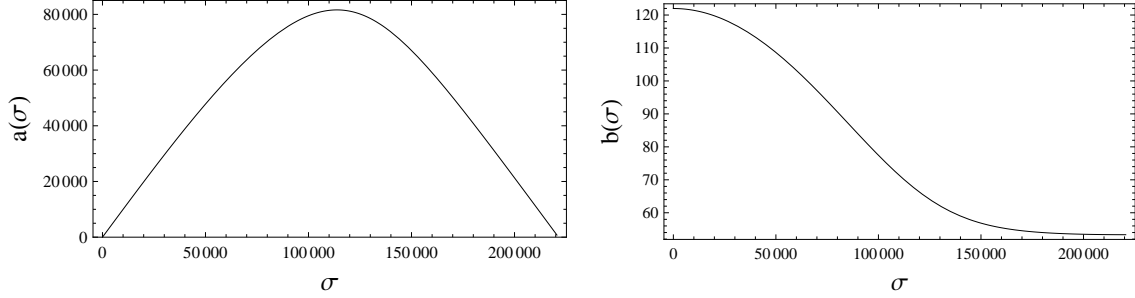


Figure 4: The 4d instanton solution for $a(\sigma)$ (left panel) and $b(\sigma)$ (right panel), all quantities given in units of G . The large numbers are due to the dynamics being sub-Planckian; see text for details.

Consider evolving the equations of motion numerically, taking the boundary conditions

$$a(\sigma) = \sigma + 2\pi G \left(\frac{n^2 \eta^2}{9b_d^2} + \frac{\kappa_2 n^4 \eta^4}{3b_d^4} + \frac{5\kappa_3 n^6 \eta^6}{9b_d^6} - \frac{\Lambda}{36\pi G} \right) \sigma^3 + \dots \quad (\text{A.8})$$

$$b(\sigma) = b_d - 2\pi G \left(\frac{2n^2 \eta^2}{3b_d} + \frac{\kappa_2 n^4 \eta^4}{b_d^3} + \frac{4\kappa_3 n^6 \eta^6}{3b_d^5} - \frac{\Lambda}{12\pi G} \right) \sigma^2 + \dots, \quad (\text{A.9})$$

in the limit $\sigma \rightarrow 0$. This corresponds to a Taylor expansion of $a(\sigma)$ and $b(\sigma)$, taking $b(0) = b_d$, and obtaining the other coefficients of the expansion by inserting into the equations of motion. Given these boundary conditions, one can show the geometry is smooth in the limit $\sigma \rightarrow 0$. We then set the value of b_d by trial and error, so that the entire solution is smooth, in particular so that as σ approaches some value σ_{\max} , $a \rightarrow \sigma_{\max} - \sigma$ and $b \rightarrow \text{constant}$. The results of such a numerical evolution are displayed in Figure 4. To generate these curves, we have used the same values of parameters as are used to generate Figures 1 and 2 in Section 2. The results agree with those of Section 2.2 in the sense that when we read off the initial and final values of the circumference of the z dimension, between the two approaches they agree.

While the interpretation of this instanton as a tunneling event is not so apparent in the 4d picture, note that the same instanton would describe the reverse “tunneling” process, the description of which is less clear in the 3d effective theory, which breaks down inside the nucleating bubble. (While we do not include the evolution here, there is no difficulty in extending the evolution of a and b to convey the evolution in the daughter vacuum.) Viewing this solution as a tunneling instanton, one can interpret it as an inflating black brane, charged with respect to the scalar field φ , nucleating in the 4d de Sitter background spacetime. Higher dimensional solutions analogous to this have been discussed by [12].

B. Bunch–Davies vacuum

To determine the power spectrum of the light scalar σ with respect to the Bunch–Davies vacuum [52], we trace the evolution of Υ_{qs}^v back into the parent vacuum and Klein-Gordon normalize the positive-frequency modes over a Cauchy surface, as is done in [53, 54, 55].

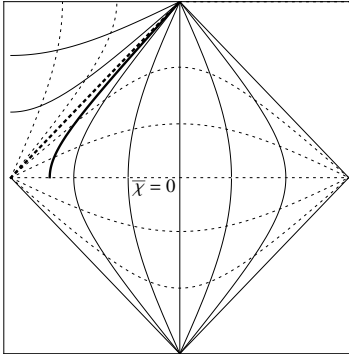


Figure 5: Conformal diagram of a de Sitter bubble nucleating in a de Sitter parent vacuum, indicating the bubble wall (thick solid curve), the future lightcone of the bubble nucleation event (thick dashed curve), some surfaces of constant η_c and $\bar{\eta}_c$ (solid curves), and some surfaces of constant χ and $\bar{\chi}$ (dashed curves). The uncharted regions of spacetime are not relevant to our discussion. The Cauchy surface $\bar{\chi} = 0$ is indicated.

Figure 5 displays a conformal diagram illustrating the geometry (the coordinates z and ϕ are suppressed). For simplicity we have constructed the diagram as if the vacuum energies inside and outside of the bubble are the same; however the statements below apply equally to more realistic geometries. We have also drawn the diagram (and we work below) as if all of spacetime can be covered by just these two universes—in other words, as if there were no other bubbles.⁴ Within the bubble, which nucleates at the middle of the left boundary and thus occupies the upper left corner of the diagram, χ is a radial coordinate on constant- z (2+1)-dimensional open FRW hypersurfaces, and η_c provides a spacelike foliation. Evidently no Cauchy surface can be drawn within the bubble.

To simplify the geometry of the parent vacuum we assume the energy density of the bubble wall does not significantly perturb the metric. Furthermore, we treat the radius b_d of the compact dimension z as if it were essentially constant throughout the parent vacuum, and we take the energy density immediately inside the bubble to be essentially equal to that of the parent vacuum on the outside (to be precise, we take $H_{\text{inf}}^2 = \Lambda/3$ to be essentially the same as the H_p^2 of (A.7)). Note that these are not necessarily good approximations of the toy compactification model described in Section 2; however they greatly simplify the computations here. In particular they allow us to treat the parent vacuum as pure de Sitter space (crossed with a circle), in which case the central, diamond-shaped region of Figure 5

⁴In fact the daughter bubble experiences an infinite number of collisions with other bubbles that nucleate in the parent vacuum [72, 73, 74, 75]; however the phenomenological success of inflationary theory suggests that any effects of such collisions should be small—linear perturbations to the standard inflationary background (at least in our past lightcone). Meanwhile, the parent vacuum itself likely resides in an open bubble, or contains other bubbles that intersect the Cauchy surface at $\bar{\chi} = 0$ (see text below). However bubble nucleation rates are likely to be exponentially suppressed, so any such disturbances would typically be very far from the physical region of interest. For simplicity we here presume both effects are negligible.

can be covered by coordinates with line element

$$ds^2 = \bar{a}^2(\bar{\eta}_c) [d\bar{\eta}_c^2 - d\bar{\chi}^2 + \cosh^2(\bar{\chi}) d\phi^2] + b_d^2 dz^2. \quad (\text{B.1})$$

Here the coordinate $\bar{\chi}$ provides the spacelike foliation, $\bar{\eta}_c$ is a spatial coordinate, and the hypersurface $\bar{\chi} = 0$ is a Cauchy surface. Since $\bar{\chi} = 0$ lies entirely within the region covered by (B.1), it is unnecessary to cover any more of the spacetime by introducing additional charts.

Note that the bubble coordinate system of (4.3) can be smoothly connected to the parent vacuum coordinate system of (B.1) by using analytic continuation,

$$\bar{\chi} = \chi - \frac{i\pi}{2}, \quad \bar{\eta}_c = \eta_c + \frac{i\pi}{2}, \quad \bar{a} = ia. \quad (\text{B.2})$$

Here the use of analytic continuation is merely a technical device to describe the propagation of modes through the bubble wall. In particular, we do not transform the coordinate of the bubble scale factor $b(\eta_c)$. Instead the z dimension of the parent vacuum maps directly onto that of the bubble (as is the case with the coordinate ϕ), assuming that $b(\eta_c) \rightarrow b_d$ and $\dot{b}_d \rightarrow 0$ as $\eta_c \rightarrow -\infty$.

Within the parent vacuum we denote the mode expansion of σ according to

$$\sigma_{vqrs}(\bar{\eta}_c, \bar{\chi}, \phi, z) = \frac{\mathcal{N}_q}{\sqrt{\bar{a}b_d}} \bar{\Upsilon}_{qs}^v(\bar{\eta}_c) \bar{U}_{qrs}(\bar{\mathbf{x}}) = \frac{\mathcal{N}_q}{\sqrt{\bar{a}b_d}} \bar{\Upsilon}_{qs}^v(\bar{\eta}_c) \bar{X}_{qr}(\bar{\chi}) \bar{\Phi}_r(\phi) \bar{Z}_s(z), \quad (\text{B.3})$$

where to simplify the presentation here and below we do not worry about keeping track of the (unimportant) overall phase. We have introduced the superfluous normalization factor \mathcal{N}_q for later convenience. The ϕ - and z -dependent Fourier modes are the same as those within the bubble, $\bar{\Phi}_r(\phi) = \Phi_r(\phi)$ and $\bar{Z}_s(z) = Z_s(z)$. Meanwhile, the $\bar{\chi}$ -dependent modes can still be written as solutions to the Legendre equation, but they now take the form

$$\bar{X}_{qr}(\bar{\chi}) = \frac{\Gamma(\frac{1}{2} + iq - r)}{\Gamma(iq)} P_{iq-1/2}^r(i \sinh(\bar{\chi})). \quad (\text{B.4})$$

The normalizations of $\bar{\Phi}_r$, \bar{Z}_s , and \bar{X}_{qr} are such that, after analytic continuation, each mode maps onto the similarly-denoted mode defined within the bubble. Note that the modes \bar{X}_{qr} , which describe the time-like evolution in the parent vacuum, correspond to positive-frequency plane waves $\propto e^{-iq\bar{\chi}}$ (up to an unimportant phase) in the limit $\bar{\chi} \rightarrow 0$.

The analytic continuation of the scale factor a gives $\bar{a} = H_{\text{inf}}^{-1} \text{sech}(\bar{\eta}_c)$, while in the parent vacuum the scale factor b is constant, $b = b_d$. This gives the equation of motion

$$\ddot{\bar{\Upsilon}}_{qs}^v + \left[q^2 + \left(\frac{3}{4} - \mu^2 \right) \text{sech}^2(\bar{\eta}_c) \right] \bar{\Upsilon}_{qs}^v = 0, \quad (\text{B.5})$$

where the dots now denote derivatives with respect to $\bar{\eta}_c$, and again $\mu = s/b_d H_{\text{inf}}$. Notice that the separation constant μ^2 appears as would a mass for the scalar field σ . The general solution of (B.5) can be written in terms of associated Legendre functions:

$$\bar{\Upsilon}_{qs}^v = \bar{C}_1^v P_{\sqrt{1-\mu^2}-1/2}^{iq}(\tanh(\bar{\eta}_c)) + \bar{C}_2^v P_{\sqrt{1-\mu^2}-1/2}^{-iq}(\tanh(\bar{\eta}_c)) \quad (\text{B.6})$$

$$\equiv \bar{C}_1^v \bar{\mathcal{F}}_1(\bar{\eta}_c) + \bar{C}_2^v \bar{\mathcal{F}}_2(\bar{\eta}_c). \quad (\text{B.7})$$

The solutions $\overline{\mathcal{F}}_1$ and $\overline{\mathcal{F}}_2$ represent two orthogonal spatial modes, and thus each should be normalized separately, with the two summed over in the final mode expansion. Hence we have introduced the index v , which distinguishes these modes. To perform the normalization it is convenient to apply a trick. Notice that (B.5) has the form of a Schrödinger equation for a point particle with position $\overline{\eta}_c$, potential energy $V(\overline{\eta}_c) = (\mu^2 - 3/4) \text{sech}^2(\overline{\eta}_c)$, and energy q^2 . The potential $V(\overline{\eta}_c)$ tends to zero as $\overline{\eta}_c \rightarrow \pm\infty$; thus $\overline{\Upsilon}_{qs}^v$ may just as well be expressed in terms of two linearly independent “scattering” solutions of the form

$$i\overline{\Upsilon}_{qs}^- \rightarrow \begin{cases} \omega_- e^{-iq\overline{\eta}_c} + e^{iq\overline{\eta}_c} & \text{as } \overline{\eta}_c \rightarrow -\infty \\ \varsigma_- e^{iq\overline{\eta}_c} & \text{as } \overline{\eta}_c \rightarrow +\infty, \end{cases} \quad (\text{B.8})$$

$$i\overline{\Upsilon}_{qs}^+ \rightarrow \begin{cases} \varsigma_+ e^{-iq\overline{\eta}_c} & \text{as } \overline{\eta}_c \rightarrow -\infty, \\ \omega_+ e^{iq\overline{\eta}_c} + e^{-iq\overline{\eta}_c} & \text{as } \overline{\eta}_c \rightarrow +\infty, \end{cases} \quad (\text{B.9})$$

where studying the Wronskian reveals $|\omega_\pm|^2 + |\varsigma_\pm|^2 = 1$, $\varsigma_+ = \varsigma_-$, and $\varsigma_+ \omega_-^* + \varsigma_-^* \omega_+ = 0$ [55]. (The factor \mathcal{N}_q was introduced in (4.4) and (B.3) to permit these simple normalizations; it will be determined later.) The normalization of the delta function is determined by noting that all of its support comes from large $|\overline{\eta}_c|$, where the solutions are plane-wave. Thus

$$\int d\overline{\eta}_c \overline{\Upsilon}_{qs}^v \overline{\Upsilon}_{q's}^{v'*} = 2\pi \delta(q - q') \delta_{vv'}, \quad (\text{B.10})$$

where the index v takes values \pm . We have introduced the modes $\overline{\Upsilon}_{qs}^\pm$ merely to take advantage of this simple normalization.

The normalized scattering solutions $\overline{\Upsilon}_{qs}^\pm$ can be expressed in terms of the solutions $\overline{\mathcal{F}}_1$ and $\overline{\mathcal{F}}_2$ by matching their asymptotic behavior onto (B.8) and (B.9). In particular, we write

$$\begin{aligned} \overline{\mathcal{F}}_1(\overline{\eta}_c) &\rightarrow \alpha_1^- e^{-iq\overline{\eta}_c} + \beta_1^- e^{iq\overline{\eta}_c} & \text{as } \overline{\eta}_c \rightarrow -\infty \\ \overline{\mathcal{F}}_1(\overline{\eta}_c) &\rightarrow \alpha_1^+ e^{-iq\overline{\eta}_c} + \beta_1^+ e^{iq\overline{\eta}_c} & \text{as } \overline{\eta}_c \rightarrow +\infty \\ \overline{\mathcal{F}}_2(\overline{\eta}_c) &\rightarrow \alpha_2^- e^{-iq\overline{\eta}_c} + \beta_2^- e^{iq\overline{\eta}_c} & \text{as } \overline{\eta}_c \rightarrow -\infty \\ \overline{\mathcal{F}}_2(\overline{\eta}_c) &\rightarrow \alpha_2^+ e^{-iq\overline{\eta}_c} + \beta_2^+ e^{iq\overline{\eta}_c} & \text{as } \overline{\eta}_c \rightarrow +\infty, \end{aligned} \quad (\text{B.11})$$

where the coefficients α_i^\pm and β_i^\pm are given by

$$\alpha_1^- = \frac{e^{-\pi q/2} \Gamma(iq)}{\Gamma(\frac{1}{2} + \sqrt{1 - \mu^2}) \Gamma(\frac{1}{2} - \sqrt{1 - \mu^2})} \quad (\text{B.12})$$

$$\beta_1^- = \frac{e^{-\pi q/2} \Gamma(-iq)}{\Gamma(\frac{1}{2} - iq + \sqrt{1 - \mu^2}) \Gamma(\frac{1}{2} - iq - \sqrt{1 - \mu^2})} \quad (\text{B.13})$$

$$\alpha_2^- = \frac{e^{\pi q/2} \Gamma(iq)}{\Gamma(\frac{1}{2} + iq + \sqrt{1 - \mu^2}) \Gamma(\frac{1}{2} + iq - \sqrt{1 - \mu^2})} \quad (\text{B.14})$$

$$\beta_2^- = \frac{e^{\pi q/2} \Gamma(-iq)}{\Gamma(\frac{1}{2} + \sqrt{1 - \mu^2}) \Gamma(\frac{1}{2} - \sqrt{1 - \mu^2})} \quad (\text{B.15})$$

$$\alpha_1^+ = 0, \quad \beta_1^+ = \frac{e^{-\pi q/2}}{\Gamma(1 - iq)}, \quad \alpha_2^+ = \frac{e^{\pi q/2}}{\Gamma(1 + iq)}, \quad \beta_2^+ = 0. \quad (\text{B.16})$$

By matching the asymptotic positive and negative “frequency” modes of $\overline{\mathcal{F}}_1$ and $\overline{\mathcal{F}}_2$ onto the asymptotic behavior of $\overline{\Upsilon}_{qs}^+$ and $\overline{\Upsilon}_{qs}^-$ given in (B.8) and (B.9), we determine

$$\overline{\Upsilon}_{qs}^-(\overline{\eta}_c) = \frac{-i\alpha_2^+ \overline{\mathcal{F}}_1(\overline{\eta}_c) + i\alpha_1^+ \overline{\mathcal{F}}_2(\overline{\eta}_c)}{\alpha_1^+ \beta_2^- - \alpha_2^+ \beta_1^-} \quad (\text{B.17})$$

$$\overline{\Upsilon}_{qs}^+(\overline{\eta}_c) = \frac{i\beta_2^- \overline{\mathcal{F}}_1(\overline{\eta}_c) - i\beta_1^- \overline{\mathcal{F}}_2(\overline{\eta}_c)}{\alpha_1^+ \beta_2^- - \alpha_2^+ \beta_1^-}. \quad (\text{B.18})$$

(Some of the terms above are zero, however we delay simplification until later.)

We have now determined all of the mode functions, up to the overall normalization \mathcal{N}_q . This is determined by enforcing Klein-Gordon normalization of the scalar field σ ,

$$\begin{aligned} (\sigma_{vqrs}, \sigma_{v'q'r's'}) &\equiv -i \int d\Sigma_\mu g^{\mu\nu} [\sigma_{vqrs} \partial_\nu \sigma_{v'q'r's'}^* - (\partial_\nu \sigma_{vqrs}) \sigma_{v'q'r's'}^*] \\ &= \delta(q - q') \delta_{rr'} \delta_{ss'} \delta_{vv'}. \end{aligned} \quad (\text{B.19})$$

As mentioned before, we set the Cauchy hypersurface Σ_μ at $\overline{\chi} = 0$. Using the orthogonality of the mode functions $\overline{\Upsilon}_{qs}^\pm$, $\overline{\Phi}_r$, and \overline{Z}_s , the above normalization condition can be written

$$2\pi |\mathcal{N}_q|^2 \cosh(\overline{\chi}) \left[\overline{X}_{qr} \partial_{\overline{\chi}} \overline{X}_{qr}^* - (\partial_{\overline{\chi}} \overline{X}_{qr}) \overline{X}_{qr}^* \right] \Big|_{\overline{\chi}=0} = i. \quad (\text{B.20})$$

The term in brackets is at first glance rather complicated; however it can be simplified with some technical manipulations, and in the end we find (up to an unimportant phase)

$$\mathcal{N}_q = \frac{1}{\sqrt{4q \sinh(\pi q)}}. \quad (\text{B.21})$$

Now that we have the Bunch–Davies modes of σ in the parent vacuum, the next step is to propagate these modes into the bubble. For the modes $\overline{\Phi}_r$ and \overline{Z}_s this is easy: they are unchanged. The modes \overline{X}_{qr} and $\overline{\Upsilon}_{qs}^\pm$ are propagated by analytic continuation of the coordinates in their arguments, as given by (B.2). The temporal mode functions $\overline{X}_{qr}(\overline{\chi})$ become the bubble spatial modes $X_{qr}(\chi)$ of (4.8). It is left to discuss the modes $\overline{\Upsilon}_{qs}^\pm$.

Note that the only dependence of the $\overline{\Upsilon}_{qs}^\pm$ on $\overline{\eta}_c$ is via $\tanh(\overline{\eta}_c)$, which is rotated into $\coth(\eta_c)$ when we take $\overline{\eta}_c \rightarrow \eta_c + i\pi/2$. The functions $\overline{\mathcal{F}}_1$ and $\overline{\mathcal{F}}_2$ thus become

$$\overline{\mathcal{F}}_1(\overline{\eta}_c) \rightarrow \tilde{\mathcal{F}}_1(\eta_c) = P^{iq} \frac{1}{\sqrt{1-\mu^2}-1/2} (\coth(\eta_c)) \quad (\text{B.22})$$

$$\overline{\mathcal{F}}_2(\overline{\eta}_c) \rightarrow \tilde{\mathcal{F}}_2(\eta_c) = P^{-iq} \frac{1}{\sqrt{1-\mu^2}-1/2} (\coth(\eta_c)). \quad (\text{B.23})$$

These are not the same as the functions \mathcal{F}_1 and \mathcal{F}_2 computed with the bubble line element (4.3), because those solutions account for the growth in the scale factor $b(\eta_c)$, whereas $\tilde{\mathcal{F}}_1$ and $\tilde{\mathcal{F}}_2$ continue from the parent vacuum where b is static. Nevertheless they have the correct asymptotic form, as $\eta_c \rightarrow -\infty$, because the scale factor $b(\eta_c) \propto \coth(\eta_c)$ approaches a constant

in that limit. All we must do is match the solutions \mathcal{F}_1 and \mathcal{F}_2 onto $\tilde{\mathcal{F}}_1$ and $\tilde{\mathcal{F}}_2$, in the limit $\eta_c \rightarrow -\infty$. In this limit, $\tilde{\mathcal{F}}_1$ and $\tilde{\mathcal{F}}_2$ have the asymptotic behavior

$$\tilde{\mathcal{F}}_1(\eta_c) \rightarrow \tilde{\alpha}_1 e^{-iq\eta_c} + \tilde{\beta}_1 e^{iq\eta_c}, \quad \tilde{\mathcal{F}}_2(\eta_c) \rightarrow \tilde{\alpha}_2 e^{-iq\eta_c} + \tilde{\beta}_2 e^{iq\eta_c}, \quad (\text{B.24})$$

where the coefficients $\tilde{\alpha}_i$ and $\tilde{\beta}_i$ are given by

$$\tilde{\alpha}_1 = e^{\pi q/2} \alpha_1^- = \frac{\Gamma(iq)}{\Gamma(\frac{1}{2} + \sqrt{1-\mu^2}) \Gamma(\frac{1}{2} - \sqrt{1-\mu^2})} \quad (\text{B.25})$$

$$\tilde{\beta}_1 = e^{-\pi q/2} \beta_1^- = \frac{e^{-\pi q} \Gamma(-iq)}{\Gamma(\frac{1}{2} - iq + \sqrt{1-\mu^2}) \Gamma(\frac{1}{2} - iq - \sqrt{1-\mu^2})} \quad (\text{B.26})$$

$$\tilde{\alpha}_2 = e^{\pi q/2} \alpha_2^- = \frac{e^{\pi q} \Gamma(iq)}{\Gamma(\frac{1}{2} + iq + \sqrt{1-\mu^2}) \Gamma(\frac{1}{2} + iq - \sqrt{1-\mu^2})} \quad (\text{B.27})$$

$$\tilde{\beta}_2 = e^{-\pi q/2} \beta_2^- = \frac{\Gamma(-iq)}{\Gamma(\frac{1}{2} + \sqrt{1-\mu^2}) \Gamma(\frac{1}{2} - \sqrt{1-\mu^2})}. \quad (\text{B.28})$$

The functions \mathcal{F}_1 and \mathcal{F}_2 have been expressed so as to have simple asymptotic behavior, see (4.17). Putting all of this together, we obtain the pair of mode functions

$$\Upsilon_{qs}^-(\eta_c) = \left(\frac{\alpha_1^+ \tilde{\alpha}_2 - \alpha_2^+ \tilde{\alpha}_1}{\alpha_1^+ \beta_2^- - \alpha_2^+ \beta_1^-} \right) i\mathcal{F}_1(\eta_c) + \left(\frac{\alpha_1^+ \tilde{\beta}_2 - \alpha_2^+ \tilde{\beta}_1}{\alpha_1^+ \beta_2^- - \alpha_2^+ \beta_1^-} \right) i\mathcal{F}_2(\eta_c) \quad (\text{B.29})$$

$$\Upsilon_{qs}^+(\eta_c) = \left(\frac{\beta_2^- \tilde{\alpha}_1 - \beta_1^- \tilde{\alpha}_2}{\alpha_1^+ \beta_2^- - \alpha_2^+ \beta_1^-} \right) i\mathcal{F}_1(\eta_c) + \left(\frac{\beta_2^- \tilde{\beta}_1 - \beta_1^- \tilde{\beta}_2}{\alpha_1^+ \beta_2^- - \alpha_2^+ \beta_1^-} \right) i\mathcal{F}_2(\eta_c). \quad (\text{B.30})$$

Referring to (B.25)–(B.28), we see that the terms in the first parantheses of (B.29) cancel to zero, as do the terms in the second parantheses of (B.30). Referring also to (B.12)–(B.16), we see that other basic simplifications are possible, and in the end we obtain

$$\Upsilon_{qs}^-(\eta_c) = ie^{-\pi q/2} \mathcal{F}_2(\eta_c) \quad (\text{B.31})$$

$$\Upsilon_{qs}^+(\eta_c) = ie^{\pi q/2} \left(\frac{\beta_1^- \alpha_2^- - \beta_2^- \alpha_1^-}{\alpha_2^+ \beta_1^-} \right) \mathcal{F}_1(\eta_c). \quad (\text{B.32})$$

The power spectrum can now be computed just as in Section 4.1, except now we must include the extra normalization factor \mathcal{N}_q . That is, we write

$$\langle \hat{\sigma}(\eta_c, q, r, s) \hat{\sigma}^\dagger(\eta_c, q', r', s') \rangle = \frac{\mathcal{N}_q^2}{a(\eta_c)b(\eta_c)} \sum_v |\Upsilon_{qs}^v(\eta_c)|^2 \delta(q - q') \delta_{rr'} \delta_{ss'}. \quad (\text{B.33})$$

As described in Section 4.1 we evaluate the power spectrum in the limit $\eta_c \rightarrow 0$, in which case the asymptotic behavior of the time-dependent parts is given by (4.18) and (4.19). Putting everything together, and performing some manipulations to eliminate some of the gamma functions, we find the power spectrum to be

$$P_{qs} = \lim_{\eta_c \rightarrow 0} \frac{\mathcal{N}_q^2}{a(\eta_c)b(\eta_c)} \sum_v |\Upsilon_{qs}^v(\eta_c)|^2 \quad (\text{B.34})$$

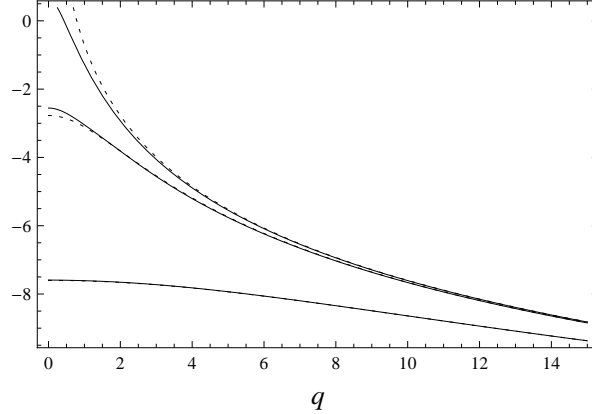


Figure 6: The power spectrum P_{qs} , expressed as $\ln(b_d P_{qs}/H_{\text{inf}})$, plotted as a function of q for $\mu = 0.1$ (top pair of curves), $\mu = 2$ (middle pair of curves), and $\mu = 10$ (bottom pair of curves). In each case we plot the actual power spectrum (solid) and the “asymptotic limit” referred to in the text (dashed).

$$\begin{aligned}
&= \frac{\pi H_{\text{inf}}}{8 b_d \sinh^2(\pi q)} \left\{ \pi \cosh(\pi q) \left| \Gamma\left(\frac{5}{4} + \frac{iq}{2} + \frac{\mu}{2}\right) \right|^{-2} \left| \Gamma\left(\frac{5}{4} + \frac{iq}{2} - \frac{\mu}{2}\right) \right|^{-2} \right. \\
&\quad \left. - \cos(\pi \sqrt{1 - \mu^2}) \text{Re} \left[\frac{2^{2iq} \Gamma(\frac{1}{2} - iq - \sqrt{1 - \mu^2}) \Gamma(\frac{1}{2} - iq + \sqrt{1 - \mu^2})}{\Gamma^2(\frac{5}{4} - \frac{iq}{2} - \frac{\mu}{2}) \Gamma^2(\frac{5}{4} - \frac{iq}{2} + \frac{\mu}{2})} \right] \right\}. \quad (\text{B.35})
\end{aligned}$$

In Figure 6 we plot the above power spectrum, and its small scale (large q, μ) asymptotic limit (4.26), for a few values of μ . It is clear that the spectrum rapidly approaches its asymptotic limit, with significant deviations only for $q \lesssim \mathcal{O}(1)$. This is not unlike the situation in regular (isotropic) 4d open bubble inflation, where the inflationary spectrum is also modified at $q \lesssim \mathcal{O}(1)$ [53, 54, 55]. In the present situation, it is evident that the deviation from the asymptotic curve is itself anisotropic; for example at $q = 2$ the curve with $\mu = 0.1$ deviates more significantly than the curve with $\mu = 10$. This anisotropy is on top of that which results from the use of anisotropic mode functions in the power spectrum.

References

- [1] A. Vilenkin, “The Birth Of Inflationary Universes,” *Phys. Rev. D* **27**, 2848 (1983).
- [2] A. D. Linde, “Eternal Chaotic Inflation,” *Mod. Phys. Lett. A* **1**, 81 (1986).
- [3] S. R. Coleman and F. De Luccia, “Gravitational Effects On And Of Vacuum Decay,” *Phys. Rev. D* **21**, 3305 (1980).
- [4] K. M. Lee and E. J. Weinberg, “Decay of the true vacuum in curved space-time,” *Phys. Rev. D* **36**, 1088 (1987).
- [5] R. Bousso and J. Polchinski, “Quantization of four-form fluxes and dynamical neutralization of the cosmological constant,” *JHEP* **0006**, 006 (2000) [arXiv:hep-th/0004134].

- [6] L. Susskind, “The anthropic landscape of string theory,” arXiv:hep-th/0302219.
- [7] M. R. Douglas, “The statistics of string / M theory vacua,” JHEP **0305**, 046 (2003) [arXiv:hep-th/0303194].
- [8] For a review, see: M. R. Douglas and S. Kachru, “Flux compactification,” Rev. Mod. Phys. **79**, 733 (2007) [arXiv:hep-th/0610102].
- [9] S. B. Giddings and R. C. Myers, “Spontaneous decompactification,” Phys. Rev. D **70**, 046005 (2004) [arXiv:hep-th/0404220].
- [10] J. J. Blanco-Pillado, D. Schwartz-Perlov and A. Vilenkin, JCAP **0912**, 006 (2009) [arXiv:0904.3106 [hep-th]].
- [11] S. M. Carroll, M. C. Johnson and L. Randall, “Dynamical compactification from de Sitter space,” arXiv:0904.3115 [hep-th].
- [12] J. J. Blanco-Pillado, D. Schwartz-Perlov and A. Vilenkin, “Transdimensional Tunneling in the Multiverse,” arXiv:0912.4082 [hep-th].
- [13] A. H. Guth, “The Inflationary Universe: A Possible Solution To The Horizon And Flatness Problems,” Phys. Rev. D **23**, 347 (1981).
- [14] J. D. Barrow and M. S. Turner, “Inflation In The Universe,” Nature **292**, 35 (1981).
- [15] R. W. Wald, “Asymptotic behavior of homogeneous cosmological models in the presence of a positive cosmological constant,” Phys. Rev. D **28**, 2118 (1983).
- [16] A. E. Gumrukcuoglu, C. R. Contaldi and M. Peloso, “CMB Anomalies from Relic Anisotropy,” arXiv:astro-ph/0608405; A. E. Gumrukcuoglu, C. R. Contaldi and M. Peloso, “Inflationary perturbations in anisotropic backgrounds and their imprint on the CMB,” JCAP **0711**, 005 (2007) [arXiv:0707.4179 [astro-ph]].
- [17] L. Ackerman, S. M. Carroll and M. B. Wise, “Imprints of a Primordial Preferred Direction on the Microwave Background,” Phys. Rev. D **75**, 083502 (2007) [arXiv:astro-ph/0701357].
- [18] T. S. Pereira, C. Pitrou and J. P. Uzan, “Theory of cosmological perturbations in an anisotropic universe,” JCAP **0709**, 006 (2007) [arXiv:0707.0736 [astro-ph]]; C. Pitrou, T. S. Pereira and J. P. Uzan, “Predictions from an anisotropic inflationary era,” JCAP **0804**, 004 (2008) [arXiv:0801.3596 [astro-ph]].
- [19] M. a. Watanabe, S. Kanno and J. Soda, “The Nature of Primordial Fluctuations from Anisotropic Inflation,” arXiv:1003.0056 [astro-ph.CO].
- [20] A. de Oliveira-Costa, M. Tegmark, M. Zaldarriaga and A. Hamilton, “The significance of the largest scale CMB fluctuations in WMAP,” Phys. Rev. D **69**, 063516 (2004) [arXiv:astro-ph/0307282].
- [21] D. J. Schwarz, G. D. Starkman, D. Huterer and C. J. Copi, “Is the low-l microwave background cosmic?,” Phys. Rev. Lett. **93**, 221301 (2004) [arXiv:astro-ph/0403353].
- [22] H. K. Eriksen, F. K. Hansen, A. J. Banday, K. M. Gorski and P. B. Lilje, “Asymmetries in the CMB anisotropy field,” Astrophys. J. **605**, 14 (2004) [Erratum-ibid. **609**, 1198 (2004)] [arXiv:astro-ph/0307507].

- [23] K. Land and J. Magueijo, “The axis of evil,” *Phys. Rev. Lett.* **95**, 071301 (2005) [arXiv:astro-ph/0502237].
- [24] T. R. Jaffe, A. J. Banday, H. K. Eriksen, K. M. Gorski and F. K. Hansen, “Evidence of vorticity and shear at large angular scales in the WMAP data: A violation of cosmological isotropy?,” *Astrophys. J.* **629**, L1 (2005) [arXiv:astro-ph/0503213]; T. R. Jaffe, A. J. Banday, H. K. Eriksen, K. M. Gorski and F. K. Hansen, “Bianchi Type VIII Models and the WMAP 3-year Data,” *Astron. Astrophys.* **460**, 393 (2006) [arXiv:astro-ph/0606046].
- [25] R. V. Buniy, A. Berera and T. W. Kephart, “Asymmetric inflation: Exact solutions,” *Phys. Rev. D* **73**, 063529 (2006) [arXiv:hep-th/0511115].
- [26] J. F. Donoghue, K. Dutta and A. Ross, “Non-isotropy in the CMB power spectrum in single field inflation,” arXiv:astro-ph/0703455.
- [27] C. Armendariz-Picon, “Creating Statistically Anisotropic and Inhomogeneous Perturbations,” *JCAP* **0709**, 014 (2007) [arXiv:0705.1167 [astro-ph]].
- [28] C. G. Boehmer and D. F. Mota, “CMB Anisotropies and Inflation from Non-Standard Spinors,” *Phys. Lett. B* **663**, 168 (2008) [arXiv:0710.2003 [astro-ph]].
- [29] T. R. Dulaney, M. I. Gresham and M. B. Wise, “Classical stability of a homogeneous, anisotropic inflating space-time,” *Phys. Rev. D* **77**, 083510 (2008) [Erratum-ibid. *D* **79**, 029903 (2009)] [arXiv:0801.2950 [astro-ph]].
- [30] A. Golovnev, V. Mukhanov and V. Vanchurin, *JCAP* **0806**, 009 (2008) [arXiv:0802.2068 [astro-ph]].
- [31] S. Yokoyama and J. Soda, “Primordial statistical anisotropy generated at the end of inflation,” *JCAP* **0808**, 005 (2008) [arXiv:0805.4265 [astro-ph]].
- [32] M. a. Watanabe, S. Kanno and J. Soda, “Inflationary Universe with Anisotropic Hair,” *Phys. Rev. Lett.* **102**, 191302 (2009) [arXiv:0902.2833 [hep-th]].
- [33] T. R. Dulaney and M. I. Gresham, “Primordial Power Spectra from Anisotropic Inflation,” arXiv:1001.2301 [astro-ph.CO].
- [34] V. F. Mukhanov, H. A. Feldman and R. H. Brandenberger, “Theory of cosmological perturbations. Part 1. Classical perturbations. Part 2. Quantum theory of perturbations. Part 3. Extensions,” *Phys. Rept.* **215**, 203 (1992).
- [35] D. H. Lyth and D. Wands, “Generating the curvature perturbation without an inflaton,” *Phys. Lett. B* **524**, 5 (2002) [arXiv:hep-ph/0110002]; T. Moroi and T. Takahashi, “Effects of cosmological moduli fields on cosmic microwave background,” *Phys. Lett. B* **522**, 215 (2001) [Erratum-ibid. *B* **539**, 303 (2002)] [arXiv:hep-ph/0110096]; K. Enqvist and M. S. Sloth, “Adiabatic CMB perturbations in pre big bang string cosmology,” *Nucl. Phys. B* **626**, 395 (2002) [arXiv:hep-ph/0109214].
- [36] A. R. Pullen and M. Kamionkowski, “Cosmic Microwave Background Statistics for a Direction-Dependent Primordial Power Spectrum,” *Phys. Rev. D* **76**, 103529 (2007) [arXiv:0709.1144 [astro-ph]].
- [37] M. Demianski and A. G. Doroshkevich, “Possible extensions of the standard cosmological model: anisotropy, rotation, and magnetic field,” *Phys. Rev. D* **75**, 123517 (2007) [arXiv:astro-ph/0702381].

- [38] M. P. Salem and J. J. Blanco-Pillado, “Signatures of anisotropic bubble nucleation,” in preparation.
- [39] Seminars delivered by M. P. Salem at the *Challenges in Theoretical Cosmology Conference* in Talloires (09/2009) and at U.C. Berkeley (12/2009), Columbia U. (01/2010), Harvard U. (02/2010), Tufts U. (02/2010), and the California Institute of Technology (02/2010).
- [40] J. Dunkley *et al.* [WMAP Collaboration], “Five-Year Wilkinson Microwave Anisotropy Probe (WMAP) Observations: Likelihoods and Parameters from the WMAP data,” arXiv:0803.0586 [astro-ph]; E. Komatsu *et al.* [WMAP Collaboration], “Five-Year Wilkinson Microwave Anisotropy Probe (WMAP) Observations: Cosmological Interpretation,” arXiv:0803.0547 [astro-ph].
- [41] E. Babichev, “Global topological k-defects,” Phys. Rev. D **74**, 085004 (2006) [arXiv:hep-th/0608071].
- [42] S. W. Hawking and I. G. Moss, “Supercooled Phase Transitions In The Very Early Universe,” Phys. Lett. B **110**, 35 (1982).
- [43] R. Kantowski and R. K. Sachs, “Some spatially homogeneous anisotropic relativistic cosmological models,” J. Math. Phys. **7**, 443 (1966).
- [44] Kip S. Thorne, “Primordial Element Formation, Primordial Magnetic Fields, and the Isotropy of the Universe,” Astrophys. J. **148**, 51 (1967).
- [45] C. B. Collins and S. W. Hawking, “The rotation and distortion of the Universe,” Mon. Not. R. Astron. Soc. **162**, 307 (1973).
- [46] A. G. Doroshkevich, V. N. Lukash, and I. D. Novikov, “Primordial radiation in an homogeneous but anisotropic universe,” Astron. Zh. **51**, 940 (1974).
- [47] J. D. Barrow, R. Juszkiewicz, and D. H. Sonoda, “Structure of the cosmic microwave background,” Nature **305**, 397 (1983).
- [48] D. H. Lyth and E. D. Stewart, “Inflationary density perturbations with $\Omega < 1$,” Phys. Lett. B **252**, 336 (1990).
- [49] See e.g. M. Abramowitz and I. Stegun, “Handbook of Mathematical Functions,” Dover (1972).
- [50] M. Bander and C. Itzykson, “Group Theory And The Hydrogen Atom. II,” Rev. Mod. Phys. **38**, 346 (1966); B. Ratra, “Spontaneously broken continuous symmetries in hyperbolic (or open de Sitter space-time,” Phys. Rev. D **50**, 5252 (1994); and references therein.
- [51] See e.g. N. D. Birrell and P. C. W. Davies, “Quantum Fields In Curved Space,” Cambridge University Press (1982).
- [52] T. S. Bunch and P. C. W. Davies, “Quantum Field Theory In De Sitter Space: Renormalization By Point Splitting,” Proc. Roy. Soc. Lond. A **360**, 117 (1978).
- [53] M. Bucher, A. S. Goldhaber and N. Turok, “An open universe from inflation,” Phys. Rev. D **52**, 3314 (1995) [arXiv:hep-ph/9411206]; M. Bucher and N. Turok, “Open Inflation With Arbitrary False Vacuum Mass,” Phys. Rev. D **52**, 5538 (1995) [arXiv:hep-ph/9503393].

- [54] M. Sasaki, T. Tanaka and K. Yamamoto, “Euclidean vacuum mode functions for a scalar field on open de Sitter space,” *Phys. Rev. D* **51**, 2979 (1995) [arXiv:gr-qc/9412025]; K. Yamamoto, M. Sasaki and T. Tanaka, “Large angle CMB anisotropy in an open universe in the one bubble inflationary scenario,” *Astrophys. J.* **455**, 412 (1995) [arXiv:astro-ph/9501109]; K. Yamamoto, M. Sasaki and T. Tanaka, “Quantum fluctuations and CMB anisotropies in one-bubble open inflation models,” *Phys. Rev. D* **54**, 5031 (1996) [arXiv:astro-ph/9605103].
- [55] J. Garriga, X. Montes, M. Sasaki and T. Tanaka, “Canonical quantization of cosmological perturbations in the one-bubble open universe,” *Nucl. Phys. B* **513**, 343 (1998) [arXiv:astro-ph/9706229]; J. Garriga, X. Montes, M. Sasaki and T. Tanaka, “Spectrum of cosmological perturbations in the one-bubble open universe,” *Nucl. Phys. B* **551**, 317 (1999) [arXiv:astro-ph/9811257].
- [56] A. A. R. Neves, L. A. Padilha, A. Fontes, E. Rodriguez, C. H. B. Cruz, L. C. Barbosa, and C. L. Cesar, “Analytical results for a Bessel function times Legendre polynomials class integrals,” *J. Phys. A: Math. Gen.* **39**, L293 (2006).
- [57] S. Winitzki, “Predictions in eternal inflation,” *Lect. Notes Phys.* **738**, 157 (2008) [arXiv:gr-qc/0612164].
- [58] A. H. Guth, *Phys. Rept.* **333**, 555 (2000); “Eternal inflation and its implications,” *J. Phys. A* **40**, 6811 (2007) [arXiv:hep-th/0702178].
- [59] B. Feldstein, L. J. Hall and T. Watari, “Density perturbations and the cosmological constant from inflationary landscapes,” *Phys. Rev. D* **72**, 123506 (2005) [arXiv:hep-th/0506235];
- [60] J. Garriga and A. Vilenkin, “Anthropic prediction for Lambda and the Q catastrophe,” *Prog. Theor. Phys. Suppl.* **163**, 245 (2006) [arXiv:hep-th/0508005].
- [61] M. L. Graesser and M. P. Salem, “The scale of gravity and the cosmological constant within a landscape,” *Phys. Rev. D* **76**, 043506 (2007) [arXiv:astro-ph/0611694].
- [62] A. A. Starobinsky, “Stochastic De Sitter (Inflationary) Stage In The Early Universe,” in: *Current Topics in Field Theory, Quantum Gravity and Strings*, Lecture Notes in Physics, eds. H. J. de Vega and N. Sanchez (Springer, Heidelberg 1986) **206**, p. 107.
- [63] A. Linde, “Sinks in the Landscape, Boltzmann Brains, and the Cosmological Constant Problem,” *JCAP* **0701**, 022 (2007) [arXiv:hep-th/0611043].
- [64] R. Bousso, “Holographic probabilities in eternal inflation,” *Phys. Rev. Lett.* **97**, 191302 (2006) [arXiv:hep-th/0605263]; R. Bousso, “Complementarity in the Multiverse,” arXiv:0901.4806 [hep-th].
- [65] A. De Simone, A. H. Guth, M. P. Salem and A. Vilenkin, “Predicting the cosmological constant with the scale-factor cutoff measure,” *Phys. Rev. D* **78**, 063520 (2008) [arXiv:0805.2173 [hep-th]]; R. Bousso, B. Freivogel and I. S. Yang, “Properties of the scale factor measure,” *Phys. Rev. D* **79**, 063513 (2009) [arXiv:0808.3770 [hep-th]]; J. Garriga and A. Vilenkin, “Holographic Multiverse,” *JCAP* **0901**, 021 (2009) [arXiv:0809.4257 [hep-th]]; A. De Simone, A. H. Guth, A. D. Linde, M. Noorbala, M. P. Salem and A. Vilenkin, “Boltzmann brains and the scale-factor cutoff measure of the multiverse,” arXiv:0808.3778 [hep-th].
- [66] B. Freivogel, M. Kleban, M. Rodriguez Martinez and L. Susskind, “Observational consequences of a landscape,” *JHEP* **0603**, 039 (2006) [arXiv:hep-th/0505232].

- [67] B. Bozek, A. J. Albrecht and D. Phillips, “Curvature Constraints from the Causal Entropic Principle,” arXiv:0902.1171 [astro-ph.CO].
- [68] R. Bousso and S. Leichenauer, “Predictions from Star Formation in the Multiverse,” arXiv:0907.4917 [hep-th].
- [69] A. De Simone and M. P. Salem, “The distribution of Ω_k from the scale-factor cutoff measure,” arXiv:0912.3783 [hep-th].
- [70] T. P. Waterhouse and J. P. Zibin, “The cosmic variance of Omega,” arXiv:0804.1771 [astro-ph]; M. Vardanyan, R. Trotta and J. Silk, “How flat can you get? A model comparison perspective on the curvature of the Universe,” arXiv:0901.3354 [astro-ph.CO].
- [71] J. J. Blanco-Pillado, M. Bucher, S. Ghassemi and F. Glanois, “When do colliding bubbles produce an expanding universe?,” Phys. Rev. D **69**, 103515 (2004) [arXiv:hep-th/0306151].
- [72] J. Garriga, A. H. Guth and A. Vilenkin, “Eternal inflation, bubble collisions, and the persistence of memory,” Phys. Rev. D **76**, 123512 (2007) [arXiv:hep-th/0612242].
- [73] A. Aguirre, M. C. Johnson and A. Shomer, “Towards observable signatures of other bubble universes,” Phys. Rev. D **76**, 063509 (2007) [arXiv:0704.3473 [hep-th]]; A. Aguirre and M. C. Johnson, “Towards observable signatures of other bubble universes II: Exact solutions for thin-wall bubble collisions,” arXiv:0712.3038 [hep-th]; A. Aguirre, M. C. Johnson and M. Tysanner, “Surviving the crash: assessing the aftermath of cosmic bubble collisions,” arXiv:0811.0866 [hep-th].
- [74] S. Chang, M. Kleban and T. S. Levi, “When Worlds Collide,” JCAP **0804**, 034 (2008) [arXiv:0712.2261 [hep-th]]; S. Chang, M. Kleban and T. S. Levi, “Watching Worlds Collide: Effects on the CMB from Cosmological Bubble Collisions,” JCAP **0904**, 025 (2009) [arXiv:0810.5128 [hep-th]].
- [75] B. Freivogel, M. Kleban, A. Nicolis and K. Sigurdson, “Eternal Inflation, Bubble Collisions, and the Disintegration of the Persistence of Memory,” arXiv:0901.0007 [hep-th].
- [76] M. P. Salem, “Bands in the sky from anisotropic bubble collisions,” arXiv:1005.5311 [hep-th].
- [77] P. W. Graham, R. Harnik and S. Rajendran, “Observing the Dimensionality of Our Parent Vacuum,” arXiv:1003.0236 [hep-th].